ARTICLE IN PRESS

Available online at www.sciencedirect.com

SCIENCE DIRECT®

Applied Ocean Research ▮ (▮▮▮▮) ▮▮▮–▮▮▮

Applied Ocean Research

www.elsevier.com/locate/apor

A coupled-mode technique for weakly nonlinear wave interaction with large floating structures lying over variable bathymetry regions

K.A. Belibassakis*, G.A. Athanassoulis

School of Naval Architecture and Marine Engineering, Section of Ship and Marine Hydrodynamics, National Technical University of Athens, Heroon Polytechniou 9, Zografos 15773, Athens, Greece

Received 18 August 2004; received in revised form 28 November 2005; accepted 20 December 2005

Abstract

A coupled-mode method is developed and applied to hydroelastic analysis of large floating platforms of shallow draft over variable bathymetry regions, characterised by parallel bottom contours. We consider the scattering problem of surface waves, under the combined effects of variable bathymetry and a semi-infinite floating elastic plate, in the time domain. The present development is based on appropriate generalisation of the unconstrained variational principle of Luke [Luke JC. A variational principle for a fluid with a free surface. J Fluid Mech 1967;27:395–7], which models the evolution of nonlinear water waves in intermediate water depth over a general bathymetry. Assuming small plate deflections and neglecting the rotation of plate section, the large floating structure has been modelled as a thin elastic plate. The present approach is based on appropriate extensions of the nonlinear coupled-mode model developed by Athanassoulis and Belibassakis [A nonlinear coupled-mode model for water waves over a general bathymetry. In: Proc. 21st international conference on offshore mechanics and arctic engineering OMAE 2002. 2002] for waves propagating in variable bathymetry regions. In order to consistently treat the wave field beneath the elastic floating plate down to the sloping bottom boundary, a complete, local-mode series expansion of the wave field is used, enhanced by appropriate sloping-bottom and free-surface modes. The latter enable consistent satisfaction of the Neumann bottom-boundary condition on a general topography, as well as the kinematical conditions on the free surface and on the elastic plate surface. By introducing this expansion into the variational principle, an equivalent coupled-mode system of horizontal equations is derived, fully accounting for the effects of nonlinearity and dispersion. Boundary conditions are also provided by the variational principle, ensuring that the edges of the plate are free of moment and shear force. Numerical results concerning floating structures lying over sloping seabeds are presented, as obtained by simplifying the fully nonlinear coupled-mode system, keeping only up to second-order terms. The present method can be extended to treat large floating elastic bodies or structures characterised by variable thickness (draft), flexural rigidity and mass distributions.

Keywords: Very large floating structures; Nonlinear hydroelastic analysis; Variable bathymetry; Coupled modes

1. Introduction

The nonlinear interaction of free-surface gravity waves with floating bodies of large dimensions is a mathematically interesting and difficult problem finding important applications. Very Large Floating Structures (VLFS), e.g., megafloats and platforms of shallow draft, have been studied intensively, being under consideration for use as floating airports and mobile offshore bases. Useful information, as well as progress on this subject, can be found in Eatock Taylor and Ohkusu [11] and Ertekin et al. [12]. Moreover, the hydroelastic analysis of VLFS is very relevant to problems concerning the interaction of water waves with ice sheets, [37]. In all these cases, hydroelasticity plays a substantial role.

Under the assumption of small slope of the free surface and of the elastic plate surface, the corresponding linearised hydroelastic problems can be effectively treated in the frequency domain. In this case, many methods have been developed, including the B-spline Galerkin method [20], Boundary Element Methods [18,19], eigenfunction expansion techniques [22,38,19], integro-differential equations [1], Wiener–Hopf techniques [39], Green–Naghdi models [23], and others; more

* Corresponding author. Tel.: +30 2107721138; fax: +30 2107721397.
E-mail addresses: kbel@fluid.mech.ntua.gr (K.A. Belibassakis), mathan@central.ntua.gr (G.A. Athanassoulis).

0141-1187/$ - see front matter
doi:10.1016/j.apor.2005.12.003

complete reviews can be found in Kashiwagi [21] and Watanabe et al. [42]. Moreover, high-frequency asymptotic methods have been developed to describe the deflection dynamics of VLFS; see, e.g., Ohkusu and Namba [33] and Hermans [17]. The latter are particularly useful in the case of short waves interacting with a deformable floating body of large horizontal dimensions.

In most applications, the water depth has been assumed to be constant, which is practically valid in the case when the horizontal dimensions of the floating structure are small in comparison with the bottom variation length, or in the case when the depth is large compared to the local wavelength (weak wave-seabed interaction). However, in cases involving the operation of VLFS in nearshore and/or coastal waters, the variations of bathymetry may have a significant effect; see, e.g. Shiraishi et al. [35]. Numerical methods for predicting the linearised hydroelastic responses of VLFS in variable bathymetry regions have also been developed, based on Boundary Element Methods (BEMs) [40,41] and Finite Element Methods (FEM) [24], on eigenfunction expansions in conjunction with step-like bottom approximation [30] and on hydroelastic local-mode series expansions [7]. Furthermore, in connection with the wave–ice sheet interaction problem, Porter and Porter [34] have recently derived an approximate, vertically integrated, mild-slope model for wave scattering by an ice sheet of variable thickness over variable bathymetry, which is valid under mild-slope assumptions with respect to the wetted surface of the ice sheet and to the bottom boundary. Although linear theory is able to provide valuable information, in many cases the effects of nonlinearity are important (as, for example, in the study of significant local slamming phenomena, Faltinsen [13], Greco et al. [16]) and should be properly taken into account. This necessitates the development of weakly and fully nonlinear models.

In the present work, a continuous, nonlinear, coupled-mode technique is developed and applied to the hydroelastic analysis of very large floating structures of shallow draft over a general bottom topography, based on an appropriate extension of the coupled-mode model developed by Athanassoulis and Belibassakis [3,4] for waves propagating in variable bathymetry regions. In contrast to the step-like bottom approximation, the present approach does not introduce artificial discontinuities (bottom corners), and has the property of converging fast. A parallel-contour bathymetry is assumed, characterised by a continuous depth function of the form $h(x, y) = h(x)$, which attains constant, but possibly different, values at the semi-infinite regions $x < a$ and $x > b$. We consider the scattering problem of surface waves, under the combined effects of variable bathymetry and a semi-infinite floating deformable structure of shallow draft, extending from $x = a$ to $x = b$; see Fig. 1. Under the assumption of small deflections and neglecting the rotation of plate section, the shallow-draft platform has been modelled as a thin floating plate, using linear elastic plate theory. On the other hand, the hydrodynamical part of the problem has been modelled on the basis of nonlinear water-wave theory.

The present development is based on an appropriate generalisation of the unconstrained variational principle of Luke [26], which models the evolution of nonlinear water waves in intermediate depth over a general bathymetry. In order to treat the wave field beneath the elastic floating structure consistently, a complete, local-mode series expansion of the wave field is used, enhanced by appropriate sloping-bottom and upper-surface modes. The latter enable consistent satisfaction of the Neumann boundary condition on a general bottom topography, as well as the kinematical conditions on the free surface and on the elastic plate surface.

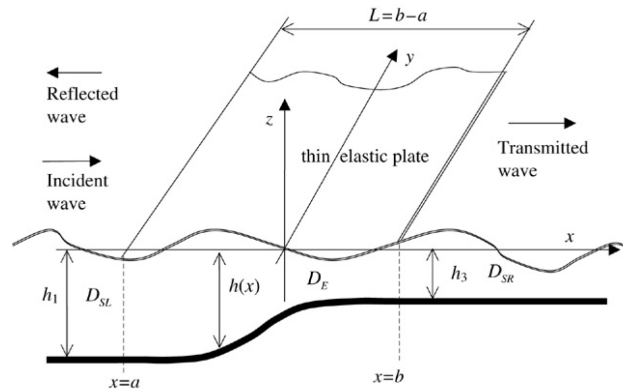

Fig. 1. Floating elastic plate in variable bathymetry region.

By introducing the local-mode series expansion into the variational principle, an equivalent coupled-mode system of horizontal equations is derived that describes the time evolution of the modal amplitudes, the free-surface elevation, and the plate deflection. The coupled-mode system accounts for the effects of wave nonlinearity and dispersion. Boundary conditions are also provided by the variational principle, ensuring that the edges of the plate are free of moment and shear force. Numerical results are presented, as obtained by simplifying the fully nonlinear coupled-mode system and keeping up to second-order terms, and compared with known solutions. Furthermore, in order to investigate the scattering effects of a large floating elastic structure in variable bathymetry regions, we examine two cases comparatively: (a) waves interacting with a sloping bottom profile; and (b) the same as before, in the presence of a floating elastic plate over the sloping bottom area.

Important aspects of the present method are that it can be extended further to treat fully three-dimensional problems, as well as floating elastic bodies or structures characterised by variable thickness (draft), flexural rigidity, and mass distributions.

2. Formulation of the problem

The environment that was studied consists of a water layer bounded above partly by the free surface and partly by a shallow-draft, large floating structure, modelled as a floating elastic plate, and below by a rigid bottom. It is assumed that the bottom surface exhibits an arbitrary one-dimensional variation in a subdomain of finite length, i.e. the bathymetry is characterised by straight and parallel bottom contours lying between two regions of constant, but possibly different, depths: $h = h_1$ (region of incidence) and $h = h_3$ (region of transmission); see Fig. 1. A Cartesian coordinate system is introduced, with its origin at some point on the mean elastic-plate surface (in the variable bathymetry region), the z-axis pointing upwards, and the y-axis parallel to the bottom contours. We consider the scattering problem of surface plane waves, under the combined effects of variable bathymetry and the semi-infinite (along the y-direction), thin, floating elastic plate, extending over the whole variable bathymetry region, from $x = a$ to $x = b$. This problem also finds applications in the case of wave interaction with ice sheets of uniform thickness in variable bathymetry.

We restrict ourselves to the two-dimensional problem corresponding to normally incident waves. However, all the analysis presented in this work can be generalised to three spatial dimensions, i.e. the two horizontal dimensions associated with the propagation space and the vertical dimension (cross space). The liquid domain is a generally shaped (non-uniform) strip D, extending to infinity in both directions $x \to \pm\infty$, bounded below by the seabed $z = -h(x)$, and above by the free surface $z = \zeta(x,t)$, for $x \in R_{SL} = \{-\infty < x < a\}$ and $x \in R_{SR} = \{b < x < \infty\}$ (in the regions of incidence and transmission, respectively), and by the elastic-plate surface, $z = w(x,t)$, for $x \in R_E = \{a \le x \le b\}$ (in the variable bathymetry region). Thus,

$$D = D(h(x), \zeta(x;t), w(x;t)) = D_{SL} \cup D_E \cup D_{SR},$$

where $D_{SL} = \{(x,z) : x \in R_{SL}, -h(x) < z < \zeta(x,t)\}$, $D_E = \{(x,z) : x \in R_E, -h(x) < z < w(x,t)\}$, and $D_{SR} = \{(x,z) : x \in R_{SR}, -h(x) < z < \zeta(x,t)\}$. All functions $h(x)$, $\zeta(x,t)$ and $w(x,t)$ are assumed bounded and smooth functions of x. Moreover, the functions $\zeta(x,t)$ and $w(x,t)$ are continuously dependent on time t, ranging over the half-line $I = \{t : t \ge 0\}$. These functions satisfy the following inequality (ensuring the connectedness of D):

$$-h(x) < \zeta(x,t), \quad \text{for } x \in R_{SL} \cup R_{SR}, \quad \text{and}$$
$$-h(x) < w(x,t), \quad \text{for } x \in R_E, \quad \text{for all } t \in I.$$

The function $h(x)$, appearing in the above definitions, represents the local depth, measured from the mean water level. It is considered to be a smooth function defined on the whole real axis R, such that $h(x) = h(a) = h_1$ for all $x \le a$, and $h(x) = h(b) = h_3$ for all $x \ge b$; see Fig. 1.

Moreover, the following assumptions are made:

$$\zeta(x = a - 0, t) = w(x = a + 0, t),$$
$$\zeta(x = b + 0, t) = w(x = b - 0, t), \quad t > 0, \tag{2.1}$$
$$\frac{\partial \zeta(x = a - 0, t)}{\partial x} = \frac{\partial w(x = a + 0, t)}{\partial x},$$
$$\frac{\partial \zeta(x = b + 0, t)}{\partial x} = \frac{\partial w(x = b - 0, t)}{\partial x}, \quad t > 0, \tag{2.2}$$

ensuring that the upper (free-surface and elastic plate) boundary remains (at all times) a smooth surface of class C^1. The first condition (2.1) expresses the natural requirement that the ends of the plate are in contact with the liquid free surface, thus excluding gaps between the free-surface elevation and the plate deflection at the plate edges. The second condition (2.2) expresses the requirement that the slope of the free surface and the slope of the elastic plate at its ends are equal. As will be discussed at the end of the next section, the latter condition is compatible with the free-surface and elastic plate kinematical conditions in the vicinity of the plate ends.

Further assumptions that are usually made (see, e.g., [42]) are that the VLFS is modelled as an elastic thin plate with free edges, and that the fluid is incompressible, inviscid and its motion is irrotational, so that a velocity potential exists. Moreover, most papers on wave response analysis of VLFS assume a linear wave. The latter assumption, however, is not valid when the wave steepness is large or when the water depth is very shallow in relation to the wavelength. Aiming to investigate the effects of wave nonlinearity, in this work we retain nonlinearity in the water-wave hydrodynamics part of the problem associated with the free-surface boundary conditions. On the other hand, in order to not add extra complexity, the irrotational flow model is used, and the large floating structure is modelled approximately on the basis of thin elastic-plate theory, assuming small plate deflections and neglecting the rotation of the plate section; see, e.g., Magrab [27] and Fung ([14], Sec. 16.8). Under these assumptions, an extension of the variational principle of Luke [26] to the hydroelastic problem that is examined is presented in the next section, governing the interaction of nonlinear water waves with floating elastic plates or ice sheets of uniform thickness in variable bathymetry regions.

3. An unconstrained variational principle for the hydroelastic problem

Under the assumptions of incompressibility and irrotationality, the non-linear problem of evolution of water waves propagating over a variable bathymetry region admits two different types of variational formulations: Hamiltonian-type, constrained on the below-the-surface kinematics [44], and unconstrained variational formulations, as e.g., the one proposed by Luke [26], in which the admissible fields are free of essential conditions, except for smoothness and completeness (compatibility) requirements.

The wave–elastic plate–seabed interaction problem also admits similar variational formulations, both Hamiltonian (see, e.g., [29,31]) and unconstrained. In the sequel, we shall present an extension of the variational principle of Luke [26] to the examined hydroelastic problem, which, in conjunction with an enhanced local-mode representation of the wave potential (presented in the next section), will serve as the basis for the derivation of an equivalent coupled-mode system of equations on the horizontal plane. To start with, we consider the following functional:

$$F[\varphi, \zeta, w] = F[\varphi(x,z,t), \zeta(x,t), w(x,t)]$$
$$= F_{SL} + F_E + F_{SR}, \tag{3.1a}$$

where

$$F_{SL}[\varphi,\zeta]=\int_{t_1}^{t_2}\int_{x=-\infty}^{x=a}\mathrm{d}x\mathrm{d}t\int_{z=-h(x)}^{z=\zeta(x,t)}\rho \times\left(\frac{\partial\varphi}{\partial t}+\frac{1}{2}\left\{\left(\frac{\partial\varphi}{\partial x}\right)^2+\left(\frac{\partial\varphi}{\partial z}\right)^2\right\}+gz\right)\mathrm{d}z, \quad (3.1b)$$

$$F_{SR}[\varphi,\zeta]=\int_{t_1}^{t_2}\int_{x=b}^{x=\infty}\mathrm{d}x\mathrm{d}t\int_{z=-h(x)}^{z=\zeta(x,t)}\rho \times\left(\frac{\partial\varphi}{\partial t}+\frac{1}{2}\left\{\left(\frac{\partial\varphi}{\partial x}\right)^2+\left(\frac{\partial\varphi}{\partial z}\right)^2\right\}+gz\right)\mathrm{d}z, \quad (3.1c)$$

$$F_{\mathrm{E}}[\varphi,w]=\int_{t_1}^{t_2}\int_{x=a}^{x=b}\mathrm{d}x\mathrm{d}t\left\{\frac{1}{2}\left(D\left(\frac{\partial^2 w}{\partial x^2}\right)^2 - m\left(\frac{\partial w}{\partial t}\right)^2\right)+\int_{z=-h(x)}^{z=w(x,t)}\rho\left(\frac{\partial\varphi}{\partial t}+\frac{1}{2}\left\{\left(\frac{\partial\varphi}{\partial x}\right)^2 + \left(\frac{\partial\varphi}{\partial z}\right)^2\right\}+gz\right)\mathrm{d}z\right\}, \quad (3.1d)$$

and $t_2>t_1\geq 0$. The parameter $D=EI$ denotes the flexural rigidity of the elastic plate (the equivalent flexural rigidity of the floating platform or the ice sheet), where E is the Young's modulus and I is the moment of inertia of the plate section (per unit length along the transverse direction). Moreover, m denotes the mass per unit area of the plate, ρ denotes the fluid density, and g is the gravitational acceleration. All the above parameters are considered to be constants. However, the present analysis can be extended to the case of variable D, m and ρ.

The only requirements imposed on the admissible function spaces are smoothness assumptions. As concerns the wave potential $\varphi(x,z,t)$, it is assumed to be of the class C^2 in D, and at least C^1 in $D\cup\partial D$. The functions $\zeta(x,t)$ and $w(x,t)$ are assumed to be appropriately smooth, obeying the continuity conditions (2.1) and (2.2).

The parts F_{SL} and F_{SR} of the functional, defined in the constant-depth water regions D_{SL} and D_{SR}, respectively, are exactly the same as in Luke's [26] functional, and are based on integration of the pressure in the liquid subdomains. The part F_E, defined in the variable bathymetry region D_E (which is bounded above by the elastic plate), consists of two terms: (i) the surface term, which is connected with the strain energy and kinetic energy of the plate, respectively (see, e.g., Gelfand and Fomin ([15], Sec. 36) Magrab ([27] Chap. 6)); and (ii) the volume term, which is again based on the integration of pressure in the liquid, in a variable bathymetry subdomain below the elastic plate. We shall now prove the following:

Theorem A. *In terms of the functional $F[\varphi,\zeta,w]$, Eq. (3.1), the examined hydroelastic problem in the variable bathymetry region, is equivalently reformulated as a variational problem of the form:*

$$\delta F[\varphi,\zeta,w]=0. \quad (3.2)$$

Proof. The variation of the functional in the left-hand side of Eq. (3.2) is obtained as the sum of variations of all terms,

$$\delta F=\delta F_{SL}+\delta F_E+\delta F_{SR} = (\delta_\varphi F_{SL}+\delta_\varphi F_E+\delta_\varphi F_{SR}) + (\delta_\zeta F_{SL}+\delta_w F_E+\delta_\zeta F_{SR}), \quad (3.3)$$

with respect to the wave potential φ and to the upper surface elevation, i.e. the free-surface elevation ζ and the elastic-plate deflection w. We now proceed to the calculation of all variations appearing in the right-hand side of Eq. (3.3). The first variation $\delta_\varphi F_{SL}$ is calculated as follows (see, e.g. [43]):

$$\delta_\varphi F_{SL}=\rho\int_{t_1}^{t_2}\int_{x=-\infty}^{x=a}\mathrm{d}t\mathrm{d}x \times\int_{z=-h(x)}^{z=\zeta(x,t)}\left(\frac{\partial\delta\varphi}{\partial t}+\frac{\partial\varphi}{\partial x}\frac{\partial\delta\varphi}{\partial x}+\frac{\partial\varphi}{\partial z}\frac{\partial\delta\varphi}{\partial z}\right)\mathrm{d}z. \quad (3.4)$$

Choosing the variation $\delta\varphi$ to vanish at infinity ($x\to\pm\infty$) and at the ends of the time interval ($t=t_{1,2}$), and changing the order of differentiation and integration, we obtain, for the first term in the right-hand side of Eq. (3.4),

$$\int_{t_1}^{t_2}\int_{x=-\infty}^{x=a}\mathrm{d}t\mathrm{d}x\int_{z=-h(x)}^{z=\zeta(x,t)}\frac{\partial\delta\varphi}{\partial t}\mathrm{d}z=\int_{t_1}^{t_2}\int_{x=-\infty}^{x=a}\mathrm{d}t\mathrm{d}x \times\left\{\frac{\partial}{\partial t}\int_{z=-h(x)}^{z=\zeta(x,t)}\delta\varphi\mathrm{d}z-\frac{\partial\zeta}{\partial t}\delta\varphi\Big|_{z=\zeta(x,t)}\right\} =-\int_{t_1}^{t_2}\int_{x=-\infty}^{x=a}\frac{\partial\zeta}{\partial t}\delta\varphi\Big|_{z=\zeta(x,t)}\mathrm{d}t\mathrm{d}x, \quad (3.5a)$$

where the integral involving the time derivative term (the first term in the brackets) is dropped because the variation $\delta\varphi$ vanishes at the ends of the time interval. For the second term in the right-hand side of Eq. (3.4), we obtain, by applying integration by parts,

$$\int_{t_1}^{t_2}\int_{x=-\infty}^{x=a}\mathrm{d}t\mathrm{d}x\int_{z=-h(x)}^{z=\zeta(x,t)}\frac{\partial\varphi}{\partial x}\frac{\partial\delta\varphi}{\partial x}\mathrm{d}z =\int_{t_1}^{t_2}\int_{x=-\infty}^{x=a}\mathrm{d}t\mathrm{d}x\left\{\frac{\partial}{\partial x}\int_{z=-h(x)}^{z=\zeta(x,t)}\frac{\partial\varphi}{\partial x}\delta\varphi\mathrm{d}z -\int_{z=-h(x)}^{z=\zeta(x,t)}\frac{\partial^2\varphi}{\partial x^2}\delta\varphi-\frac{\partial\zeta}{\partial x}\frac{\partial\varphi}{\partial x}\delta\varphi\Big|_{z=\zeta(x,t)} +\left(-\frac{\mathrm{d}h}{\mathrm{d}x}\frac{\partial\varphi}{\partial x}\delta\varphi\Big|_{z=-h(x)}\right)\right\}$$
$$=\int_{t_1}^{t_2}\mathrm{d}t\left(\int_{z=-h(x)}^{z=\zeta(x,t)}\mathrm{d}z\frac{\partial\varphi}{\partial x}\delta\varphi\Big|_{x=a}+\int_{x=-\infty}^{x=a}\mathrm{d}x \times\left\{-\int_{z=-h(x)}^{z=\zeta(x,t)}\frac{\partial^2\varphi}{\partial x^2}\delta\varphi\mathrm{d}z-\frac{\partial\zeta}{\partial x}\frac{\partial\varphi}{\partial x}\delta\varphi\Big|_{z=\zeta(x,t)} +\left(-\frac{\mathrm{d}h}{\mathrm{d}x}\frac{\partial\varphi}{\partial x}\delta\varphi\Big|_{z=-h(x)}\right)\right\}\right) \quad (3.5b)$$

and, for the third term,

$$\int_{t_1}^{t_2}\int_{x=-\infty}^{x=a}\mathrm{d}t\mathrm{d}x\int_{z=-h(x)}^{z=\zeta(x,t)}\frac{\partial\varphi}{\partial z}\frac{\partial\delta\varphi}{\partial z}\mathrm{d}z=\int_{t_1}^{t_2}\int_{x=-\infty}^{x=a}\mathrm{d}t\mathrm{d}x \times\left\{\left[\frac{\partial\varphi}{\partial z}\delta\varphi\right]_{z=-h(x)}^{z=\zeta(x,t)}-\int_{z=-h(x)}^{z=\zeta(x,t)}\frac{\partial^2\varphi}{\partial z^2}\delta\varphi\mathrm{d}z\right\}$$

$$= \int_{t_1}^{t_2} \int_{x=-\infty}^{x=a} \mathrm{d}t\mathrm{d}x \left\{ \frac{\partial\varphi}{\partial z}\delta\varphi\bigg|_{z=\zeta(x,t)} - \frac{\partial\varphi}{\partial z}\delta\varphi\bigg|_{z=-h(x)} - \int_{z=-h(x)}^{z=\zeta(x,t)} \frac{\partial^2\varphi}{\partial z^2}\delta\varphi\mathrm{d}z \right\}. \tag{3.5c}$$

Collecting together all terms, Eqs. (3.4) and (3.5), the variation $\delta_\varphi F_{SL}$ finally becomes:

$$\begin{aligned}\delta_\varphi F_{SL} = {}& \rho\int_{t_1}^{t_2}\mathrm{d}t\int_{z=-h(x)}^{\zeta(x,t)} \frac{\partial\varphi}{\partial x}\delta\varphi\bigg|_{x=a}\mathrm{d}z \\ &- \rho\int_{t_1}^{t_2}\int_{x=-\infty}^{x=a}\mathrm{d}x\mathrm{d}t\int_{z=-h(x)}^{z=\zeta(x,t)}\mathrm{d}z\left(\frac{\partial^2\varphi}{\partial x^2}+\frac{\partial^2\varphi}{\partial z^2}\right)\delta\varphi \\ &- \rho\int_{t_1}^{t_2}\int_{x=-\infty}^{x=a}\mathrm{d}t\mathrm{d}x\left(\frac{\partial\zeta}{\partial t}+\frac{\partial\zeta}{\partial x}\frac{\partial\varphi}{\partial x}-\frac{\partial\varphi}{\partial z}\right)\delta\varphi\bigg|_{z=\zeta(x,t)} \\ &- \rho\int_{t_1}^{t_2}\int_{x=-\infty}^{x=a}\mathrm{d}t\mathrm{d}x\left(\frac{\partial h}{\partial x}\frac{\partial\varphi}{\partial x}+\frac{\partial\varphi}{\partial z}\right)\delta\varphi\bigg|_{z=-h(x)}. \end{aligned}\tag{3.6}$$

Working similarly, we obtain, for $\delta_\varphi F_{SR}$,

$$\begin{aligned}\delta_\varphi F_{SR} = {}& -\rho\int_{t_1}^{t_2}\mathrm{d}t\int_{z=-h(z)}^{\zeta(x,t)} \frac{\partial\varphi}{\partial x}\delta\varphi\bigg|_{x=b}\mathrm{d}z \\ &- \rho\int_{t_1}^{t_2}\int_{x=b}^{x=\infty}\mathrm{d}x\mathrm{d}t\int_{z=-h(x)}^{z=\zeta(x,t)}\mathrm{d}z\left(\frac{\partial^2\varphi}{\partial x^2}+\frac{\partial^2\varphi}{\partial z^2}\right)\delta\varphi \\ &- \rho\int_{t_1}^{t_2}\int_{x=b}^{x=\infty}\mathrm{d}t\mathrm{d}x\left(\frac{\partial\zeta}{\partial t}+\frac{\partial\zeta}{\partial x}\frac{\partial\varphi}{\partial x}-\frac{\partial\varphi}{\partial z}\right)\delta\varphi\bigg|_{z=\zeta(x,t)} \\ &- \rho\int_{t_1}^{t_2}\int_{x=b}^{x=\infty}\mathrm{d}t\mathrm{d}x\left(\frac{\partial h}{\partial x}\frac{\partial\varphi}{\partial x}+\frac{\partial\varphi}{\partial z}\right)\delta\varphi\bigg|_{z=-h(x)}, \end{aligned}\tag{3.7}$$

and, for $\delta_\varphi F_E$,

$$\begin{aligned}\delta_\varphi F_E = {}& \rho\int_{t_1}^{t_2}\mathrm{d}t\int_{z=-h(x)}^{w(x,t)}\left[\frac{\partial\varphi}{\partial x}\delta\varphi\right]_{x=a}^{x=b}\mathrm{d}z \\ &- \rho\int_{t_1}^{t_2}\int_{x=b}^{x=\infty}\mathrm{d}x\mathrm{d}t\int_{z=-h(x)}^{z=w(x,t)}\mathrm{d}z\left(\frac{\partial^2\varphi}{\partial x^2}+\frac{\partial^2\varphi}{\partial z^2}\right)\delta\varphi \\ &- \rho\int_{t_1}^{t_2}\int_{x=a}^{x=b}\mathrm{d}t\mathrm{d}x\left(\frac{\partial w}{\partial t}+\frac{\partial w}{\partial x}\frac{\partial\varphi}{\partial x}-\frac{\partial\varphi}{\partial z}\right)\delta\varphi\bigg|_{z=w(x,t)} \\ &- \rho\int_{t_1}^{t_2}\int_{x=a}^{x=b}\mathrm{d}t\mathrm{d}x\left(\frac{\partial h}{\partial x}\frac{\partial\varphi}{\partial x}+\frac{\partial\varphi}{\partial z}\right)\delta\varphi\bigg|_{z=-h(x)}. \end{aligned}\tag{3.8}$$

We now proceed to the calculation of the terms associated with the variation of the free-surface ζ and the plate deflection w (the terms in the last parentheses in the right-hand side of Eq. (3.3)). The variations $\delta_\zeta F_{SL}$ and $\delta_\zeta F_{SR}$ are easily obtained as follows:

$$\delta_\zeta F_{SL} = \rho\int_{t_1}^{t_2}\int_{x=-\infty}^{x=a}\mathrm{d}x\mathrm{d}t\left\{\left(\frac{\partial\varphi}{\partial t}+\frac{1}{2}\left(\left(\frac{\partial\varphi}{\partial x}\right)^2+\left(\frac{\partial\varphi}{\partial z}\right)^2\right)\right)_{z=\zeta(x,t)}+g\zeta\right\}\delta\zeta, \tag{3.9a}$$

$$\delta_\zeta F_{SR} = \rho\int_{t_1}^{t_2}\int_{x=b}^{x=\infty}\mathrm{d}x\mathrm{d}t\left\{\left(\frac{\partial\varphi}{\partial t}+\frac{1}{2}\left(\left(\frac{\partial\varphi}{\partial x}\right)^2+\left(\frac{\partial\varphi}{\partial z}\right)^2\right)\right)_{z=\zeta(x,t)}+g\zeta\right\}\delta\zeta. \tag{3.9b}$$

The variation $\delta_w F_E$, with respect to the variation of the plate deflection δw, is given by

$$\begin{aligned}\delta_w F_E = {}& \rho\int_{t_1}^{t_2}\int_{x=a}^{x=b}\mathrm{d}x\mathrm{d}t \\ &\times\left\{\left(\frac{\partial\varphi}{\partial t}+\frac{1}{2}\left(\left(\frac{\partial\varphi}{\partial x}\right)^2+\left(\frac{\partial\varphi}{\partial z}\right)^2\right)\right)_{z=w(x,t)}+gw\right\}\delta w \\ &+\int_{t_1}^{t_2}\int_{x=a}^{x=b}\mathrm{d}x\mathrm{d}t\left(-m\frac{\partial w}{\partial t}\frac{\partial\delta w}{\partial t}+D\frac{\partial^2 w}{\partial x^2}\frac{\partial^2\delta w}{\partial x^2}\right),\end{aligned}$$

and, after applying integration by parts to the last two terms, we obtain

$$\begin{aligned}\delta_w F_E = {}& \int_{t_1}^{t_2}\int_{x=a}^{x=b}\mathrm{d}x\mathrm{d}t \\ &\times\left\{\left(\rho\frac{\partial\varphi}{\partial t}+\frac{\rho}{2}\left(\left(\frac{\partial\varphi}{\partial x}\right)^2+\left(\frac{\partial\varphi}{\partial z}\right)^2\right)\right)_{z=w(x,t)}+\rho gw\right\} \\ &\times\delta w - m\int_{x=a}^{x=b}\left[\frac{\partial w}{\partial t}\delta w\right]_{t=t_1}^{t=t_2}\mathrm{d}x \\ &+D\int_{t_1}^{t_2}\mathrm{d}t\left\{\left[\frac{\partial^2 w}{\partial x^2}\delta\left(\frac{\partial w}{\partial x}\right)-\frac{\partial^3 w}{\partial x^3}\delta w\right]_{x=a}^{x=b}\right. \\ &\left.+\int_{x=a}^{x=b}\mathrm{d}x\left(m\frac{\partial^2 w}{\partial t^2}+D\frac{\partial^4 w}{\partial x^4}\right)\delta w\right\}.\end{aligned}$$

In addition, assuming that the variations δw vanish at $t = t_1$ and $t = t_2$ (i.e., at the beginning and end of the time interval), the second integral in the right-hand side of the above equation becomes zero, resulting in

$$\begin{aligned}\delta_w F_E = {}& \int_{t_1}^{t_2}\int_{x=a}^{x=b}\mathrm{d}x\mathrm{d}t\left\{m\frac{\partial^2 w}{\partial t^2}+D\frac{\partial^4 w}{\partial x^4}\right. \\ &\left.+\rho\left(\frac{\partial\varphi}{\partial t}+\frac{1}{2}\left(\left(\frac{\partial\varphi}{\partial x}\right)^2+\left(\frac{\partial\varphi}{\partial z}\right)^2\right)\right)_{z=w(x,t)}+\rho gw\right\} \\ &\times\delta w + D\int_{t_1}^{t_2}\left[\frac{\partial^2 w}{\partial x^2}\delta\left(\frac{\partial w}{\partial x}\right)-\frac{\partial^3 w}{\partial x^3}\delta w\right]_{x=a}^{x=b}\mathrm{d}t.\end{aligned}\tag{3.10}$$

Gathering together all terms, and considering the variation of each part of the functional F, Eq. (3.3), independent of the others, it can be seen that the condition of stationarity of the functional F is equivalent to the hydroelastic problem studied. More precisely, the variational equations $\delta_\varphi F_{SL} = \delta_\varphi F_{SR} = 0$ model the *water-wave kinematics* in the two half-strips D_{SL} and D_{SR}, respectively:

$$\Delta\varphi = 0, \quad -\infty < x < a \quad \text{and} \quad b < x < +\infty, \quad -h(x) < z < \zeta(x,t), \tag{3.11a}$$

$$\frac{\partial \zeta}{\partial t} + \frac{\partial \zeta}{\partial x}\frac{\partial \varphi}{\partial x} - \frac{\partial \varphi}{\partial z} = 0, \quad \text{on } z = \zeta(x,t), \tag{3.11b}$$

$$\frac{\partial h}{\partial x}\frac{\partial \varphi}{\partial x} + \frac{\partial \varphi}{\partial z} = 0, \quad \text{on } z = -h(x), \tag{3.11c}$$

where $\Delta = \frac{\partial^2}{\partial x^2} + \frac{\partial^2}{\partial z^2}$ denotes the Laplacian on the vertical (xz) plane. The equation $\delta_\varphi F_E = 0$ models *the wave kinematics in the elastic plate region*:

$$\Delta\varphi = 0, \quad a < x < b, \quad -h < z < w(x,t), \tag{3.12a}$$

$$\frac{\partial w}{\partial t} + \frac{\partial w}{\partial x}\frac{\partial \varphi}{\partial x} - \frac{\partial \varphi}{\partial z} = 0, \quad \text{on } z = w(x;t), \tag{3.12b}$$

$$\frac{\partial h}{\partial x}\frac{\partial \varphi}{\partial x} + \frac{\partial \varphi}{\partial z} = 0, \quad \text{on } z = -h(x). \tag{3.12c}$$

Moreover, the equations $\delta_\zeta F_{SL} = \delta_\zeta F_{SR} = 0$ model the *free-surface dynamics* (Bernoulli's integral) on the upper boundary of the two half-strips D_{SL} and D_{SR}, respectively:

$$\frac{1}{2}\left(\left(\frac{\partial \varphi}{\partial x}\right)^2 + \left(\frac{\partial \varphi}{\partial z}\right)^2\right) + \frac{\partial \varphi}{\partial t} + g\zeta = 0,$$
$$-\infty < x < a \text{ and } b < x < \infty, \quad \text{on } z = \zeta(x,t). \tag{3.13a}$$

Finally, from Eq. (3.10), expressing $\delta_w F_E = 0$ by considering (i) the variation of the plate deflection δw at the interior points of the interval $a < x < b$, (ii) the variation δw at the end-points $x = a$ and $x = b$, and (iii) the variation $\delta(\frac{\partial w}{\partial x})$ in the slope of the deflection at the end-points $x = a$ and $x = b$ to be independent, we obtain the equations and boundary conditions modelling the (semi-linearised) *elastic-plate dynamics*. More specifically, from the term associated with the variation $\delta w(x;t)$, $a < x < b$, we obtain the elastic plate equation:

$$\rho\left(\frac{\partial \varphi}{\partial t} + \frac{1}{2}\left(\left(\frac{\partial \varphi}{\partial x}\right)^2 + \left(\frac{\partial \varphi}{\partial z}\right)^2\right) + gw\right) + m\frac{\partial^2 w}{\partial t^2}$$
$$+ D\frac{\partial^4 w}{\partial x^4} = 0, \quad a < x < b, \quad \text{on } z = w(x,t). \tag{3.13b}$$

Also, from the terms of $\delta_w F_E$ associated with the variations $\delta w(x=a,t)$, $\delta w(x=b,t)$, $\delta\left(\frac{\partial w(x=a,t)}{\partial x}\right)$ and $\delta\left(\frac{\partial w(x=b,t)}{\partial x}\right)$, at the plate ends, we obtain the following edge conditions, respectively:

$$\frac{\partial^3 w(x=a+0,t)}{\partial x^3} = 0, \quad \text{and} \tag{3.14a}$$

$$\frac{\partial^3 w(x=b-0,t)}{\partial x^3} = 0, \tag{3.14b}$$

$$\frac{\partial^2 w(x=a+0,t)}{\partial x^2} = 0 \quad \text{and} \tag{3.15a}$$

$$\frac{\partial^2 w(x=b-0,t)}{\partial x^2} = 0. \tag{3.15b}$$

Eqs. (3.14) and (3.15) ensure that the elastic plate, at the ends $x = a$ and $x = b$, is free of shear force and moment, respectively. This concludes the proof of Theorem A.

In concluding this section, we shall make some comments concerning the compatibility of condition (2.2), requiring the continuity of the free-surface slope and the plate slope at the plate ends, with the kinematical conditions (3.11b) and (3.12b) on the upper boundary. Without loss of generality, we consider the latter conditions only at the left end-point of the plate. Using Eq. (3.11b) at $x = a - 0$ and Eq. (3.12b) at $x = a + 0$, in conjunction with the C^2-continuity of the wave potential $\varphi(x,z,t)$, for $(x,z) \in D$ and all $t > 0$, we obtain

$$\left(\frac{\partial w(a+0,t)}{\partial t} - \frac{\partial \zeta(a-0,t)}{\partial t}\right)$$
$$+ \left(\frac{\partial w(a+0,t)}{\partial x} - \frac{\partial \zeta(a-0,t)}{\partial x}\right)\frac{\partial \varphi(a,z=\zeta,t)}{\partial x} = 0.$$

However, the first term in the left-hand side of the above equation vanishes by virtue of assumption (2.1). Using the fact that the horizontal flow velocity $\frac{\partial \varphi(a,z=\zeta,t)}{\partial x}$ at the plate end is generally non-zero, we obtain condition (2.2).

On the basis of conditions (2.1) and (2.2), we shall proceed to our analysis by using the unified notation

$$\eta(x,t) = \begin{cases} \zeta(x,t), & -\infty < x < a \text{ and } b < x < \infty \\ w(x,t), & a \le x \le b \end{cases} \tag{3.16}$$

expressing the elevation of the upper boundary of the whole liquid domain D.

4. Local-mode representation

In this section, a complete, local-mode series expansion of the wave potential φ, valid in both the two half-strips D_{SL} and D_{SR}, and in the variable bathymetry region containing the elastic plate D_E, is presented. This representation has the general form

$$\varphi(x,z,t) = \sum_n \varphi_n(x,t) Z_n(z, h(x), \eta(x,t)),$$

and has been derived by Athanassoulis and Belibassakis [3,4] with application to the problem of nonlinear water waves propagating over variable bathymetry regions. The usefulness of the above representation is that, substituted in the variational equation (3.2), it leads to a nonlinear, coupled-mode system of differential equations on the horizontal plane, with respect to unknown modal amplitudes $\varphi_n(x,t)$ and the unknown elevation $\eta(x,t)$. The coupled-mode system greatly facilitates the numerical solution of the present hydroelastic problem and its derivation will be presented in the next section.

A similar modal-type series expansion has been introduced earlier by Nadaoka et al. [32] for the development of a fully dispersive, weakly nonlinear, multiterm-coupling model for water waves, with application to slowly varying bottom topography. In that work, the vertical modes have been selected to have the form $\cosh(k_n(z+h))\cosh^{-1}(k_n h)$, with $k_n > 0$, thus being independent from the upper surface elevation $\eta(x,t)$. As will be described in more detail in the sequel, the major part of the present set of vertical modes $\{Z_n(z,h,\eta), n = 0,1,2,\ldots\}$ is obtained by solving a Sturm–Liouville problem, formulated at the local vertical interval $-h(x) < z < \eta(x,t)$, ensuring L_2-completeness. This set contains both hyperbolic and trigonometric functions, dependent on both the local depth $h(x)$ and the (instantaneous) upper surface elevation $\eta(x,t)$. However, the boundary conditions satisfied by these local vertical eigenfunctions are not compatible with the boundary conditions of the problem at the bottom surface, if the bottom is not horizontal or mildly sloping, and at the upper surface. In order to overcome the mild-slope bottom approximation and to satisfy the upper-surface boundary conditions consistently, the present set has been enhanced by including the two additional modes $\{Z_{-2}(z,h,\eta), Z_{-1}(z,h,\eta)\}$ with unknown amplitudes $\{\varphi_{-2}(x,t), \varphi_{-1}(x,t)\}$. The latter are the additional degrees of freedom required for the consistent satisfaction of the upper-surface and the sloping-bottom boundary conditions, respectively. The idea of the sloping-bottom mode has been presented by Athanassoulis and Belibassakis [2] for the propagation of linearised waves in general bathymetry regions. The latter work has been extended to second-order Stokes waves (in the frequency domain) by Belibassakis and Athanassoulis [6], where the necessity of a free-surface additional mode has also been discussed for the satisfaction of the (second-order) free-surface boundary condition.

We now proceed to state and prove the following:

Theorem B. *Consider the generally shaped (non-uniform) strip D, extending to infinity in both directions $x \to \pm\infty$ and bounded by the graphs of the functions $z = -h(x)$ ("lower" boundary, seabed) and $z = \eta(x,t)$ ("upper" boundary); see Fig. 2. Let $\varphi(x,z,t)$, defined on $D \times I$, be a twice continuously differentiable function in D with continuous first spatial derivatives up to and including the boundary ∂D, for all $t \in I$. Moreover, $\varphi(x,z;t)$ is considered to be continuously differentiable with respect to $t \in I$, for each $(x,z) \in D \cup \partial D$. Then, the field $\varphi(x,z,t)$, standing for the wave potential, admits the following, uniformly convergent, local-mode series expansion:*

$$\varphi(x,z,t) = \sum_{n=-2}^{\infty} \varphi_n(x,t) Z_n(z,h(x),\eta(x,t)), \tag{4.1}$$

where

$$Z_{-2}(z,h,\eta) = \frac{\mu_0 h_0 + 1}{2(\eta+h)h_0}(z+h)^2 - \frac{\mu_0 h_0 + 1}{2h_0}(\eta+h) + 1, \tag{4.2}$$

represents the vertical structure of the term $\varphi_{-2}Z_{-2}$, which will be called the upper-surface mode,

$$Z_{-1}(z,h,\eta) = \frac{\mu_0 h_0 - 1}{2h_0(\eta+h)}(z+h)^2 + \frac{1}{h_0}(z+h) + \frac{2h_0 - (\eta+h)(\mu_0 h_0 + 1)}{2h_0}, \tag{4.3}$$

represents the vertical structure of the term $\varphi_{-1}Z_{-1}$, which will be called the sloping-bottom mode, *and*

$$Z_0(z,h,\eta) = \frac{\cosh[k_0(z+h)]}{\cosh[k_0(\eta+h)]}, \qquad \text{and}$$

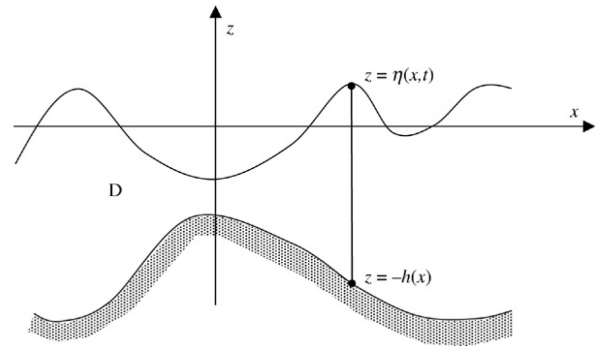

Fig. 2. Shapshot of the flow domain.

$$Z_n(z,h,\eta) = \frac{\cos[k_n(z+h)]}{\cos[k_n(\eta+h)]}, \quad n = 1,2,3,\ldots \tag{4.4}$$

are the corresponding functions associated with the rest of the terms, which will be called the propagating ($\varphi_0 Z_0$) *and* evanescent ($\varphi_n Z_n$, $n = 1,2,\ldots$) *modes.*

The (numerical) parameters $\mu_0, h_0 > 0$ are positive constants, not subjected to any a priori restrictions. Moreover, the z-independent quantities $k_n = k_n(h,\eta)$, $n = 0,1,2\ldots$, appearing in Eq. (4.4) are defined as the positive roots of the transcendental equations,

$$\mu_0 - k_0 \tanh[k_0(h+\eta)] = 0, \qquad \text{and}$$
$$\mu_0 + k_n \tan[k_n(h+\eta)] = 0, \quad n = 1,2,3,\ldots. \tag{4.5}$$

Proof. Consider the restriction $f(z)$ of the wave potential $\varphi(x,z;t)$ at any vertical section $x = \text{const}$ and for any time instant $t \in I$; see Fig. 2. Obviously, this function, defined on the vertical interval $-h(x) \le z \le \eta(x,t)$, is a smooth one $f(z) \in \{C^2(J) \cap C^1(\bar{J})\}$, where $J = \{-h(x) < z < \eta(x,t)\}$ and $\bar{J} = J \cup \partial J$. Let us now define the following mixed derivative of $f(z)$ at the upper end $z = \eta(x,t)$:

$$f'_\eta = \left.\frac{\partial\varphi(x,z,t)}{\partial z}\right|_{z=\eta(x,t)} - \mu_0 \varphi(x,z,t)|_{z=\eta(x,t)}, \tag{4.6}$$

where $\mu_0 = \omega_0^2/g$ is a fixed frequency-type parameter. As mentioned already, this parameter is not subjected to any a priori restriction, and can be selected arbitrarily. (An appropriate choice for this parameter is to be selected on the basis of the central frequency, ω_0, of the waveform propagating in D.)

Except for the case of linearised (infinitesimal amplitude) monochromatic waves of frequency $\omega = \omega_0$, the derivative $f'_\eta = f'_\eta(x,t)$ is generally non-zero. From its definition, Eq. (4.6), it is expected to be a continuously differentiable function with respect to both x and t.

Let us also consider the vertical derivative of $f(z)$ at the bottom surface $z = -h(x)$:

$$f'_h = \left.\frac{\partial\varphi(x,z,t)}{\partial z}\right|_{z=-h(x)}. \tag{4.7}$$

Except for the case of waves propagating in a uniform-depth strip ($h(x) = h = \text{const}$), $f'_h = f'_h(x,t)$ is generally non-zero.

From its definition, Eq. (4.7), it follows that this function is also a continuously differentiable function with respect to both x and t.

These two quantities $f'_\eta(x,t)$ and $f'_h(x,t)$ are unknown in the general case of waves propagating in the variable bathymetry region. We define the upper-surface and the sloping-bottom mode amplitudes ($\varphi_n, n = -2, -1$), to be given by:

$$\varphi_{-2}(x,t) = h_0 f'_\eta(x,t), \tag{4.8a}$$

$$\varphi_{-1}(x,t) = h_0 f'_h(x,t), \tag{4.8b}$$

where h_0 is an appropriate scaling parameter that can also be selected arbitrarily. (An appropriate choice for this parameter is the average depth of the variable bathymetry domain D.)

By noticing the vertical structure of these modes, given by Eqs. (4.2) and (4.3), we easily see that the *reduced potential*

$$\varphi_R(x,z,t) = \varphi(x,z,t) - \varphi_{-2}(x,t)Z_{-2}(z,\eta,h) - \varphi_{-1}(x,t)Z_{-1}(z,\eta,h), \tag{4.9}$$

is a twice continuously differentiable function, $\varphi_R \in C^2(D \times I) \cap C^1(\bar{D} \times I)$, which, for all x and t, at the upper surface and at the bottom surface satisfies the following conditions:

$$\left.\frac{\partial \varphi_R(x,z,t)}{\partial z}\right|_{z=\eta(x,t)} - \mu_0 \varphi_R(x,z,t)|_{z=\eta(x,t)} = 0, \tag{4.10a}$$

$$\left.\frac{\partial \varphi_R(x,z,t)}{\partial z}\right|_{z=-h(x)} = 0. \tag{4.10b}$$

The above conditions are sufficient to ensure the representation of $\varphi_R(x,z,t)$, at any vertical section ($x = \text{const}$) and any time ($t = \text{const}$), in the form of the eigenfunction expansion,

$$\varphi_R(x,z,t) = \sum_{n=0}^{\infty} \varphi_n(x,t) Z_n(z,h(x),\eta(x,t)), \tag{4.11}$$

where the set of vertical functions $\{Z_n(z,h(x),\eta(x,t)), n = 0,1,2,3\ldots\}$ and the set of numbers $\{k_n, n = 0,1,2,3\ldots\}$, given by Eqs. (4.4) and (4.5), respectively, are obtained as the solution of the local (for each x and t) Sturm–Liouville problem:

$$\frac{\partial^2 Z_n}{\partial z^2} - k_n^2 Z_n = 0, \quad -h(x) < z < \eta(x;t), \tag{4.12a}$$

$$\left.\frac{\partial Z_n(z)}{\partial z}\right|_{z=\eta(x,t)} - \mu_0 Z_n(z)|_{z=\eta(x,t)} = 0, \tag{4.12b}$$

$$\left.\frac{\partial Z_n(z)}{\partial z}\right|_{z=-h(x)} = 0. \tag{4.12c}$$

From the properties of regular eigenvalue problems (see e.g., [9]), the set of eigenfunctions $\{Z_n(z,h,\eta), n = 0,1,2,3\ldots\}$ constitutes an L_2-basis in the z-interval $-h(x) < z < \eta(x,t)$, for each x and t. Moreover, since the function $\varphi_R(x,z;t)$ fulfils the same boundary conditions, Eqs. (4.10), as the eigenfunctions, Eqs. (4.12b) and (4.12c), the series (4.11) converges uniformly to the function $\varphi_R(x,z;t)$. Then, by using Eq. (4.9) in Eq. (4.11) and passing the newly introduced modes $\varphi_n Z_n, n = -2,-1$, to the right-hand side, we obtain the enhanced local-mode representation given by Eq. (4.1), and the theorem is proved. □

Remarks. (i) For the representation (4.1) to be valid, the vertical structure of each of the two additional modes, $Z_n(z,h,\eta), n = -2,-1$, needs to be a smooth function satisfying

$$\left.\frac{\partial Z_{-2}(z)}{\partial z}\right|_{z=\eta(x,t)} - \mu_0 Z_{-2}(z)|_{z=\eta(x,t)} = \alpha \neq 0,$$

$$\left.\frac{\partial Z_{-2}(z)}{\partial z}\right|_{z=-h(x)} = 0,$$

and

$$\left.\frac{\partial Z_{-1}(z)}{\partial z}\right|_{z=\eta(x,t)} - \mu_0 Z_{-1}(z)|_{z=\eta(x,t)} = 0,$$

$$\left.\frac{\partial Z_{-1}(z)}{\partial z}\right|_{z=-h(x)} = \beta \neq 0,$$

respectively. The particular choices given by Eqs. (4.2) and (4.3) are simply least-degree polynomials satisfying exactly the above requirements (with $\alpha = \beta = \frac{1}{h_0}$), which, in addition, have been normalised:

$$Z_{-2}(z)|_{z=\eta(x,t)} = Z_{-1}(z)|_{z=\eta(x,t)} = 1,$$

in order to be compatible with the eigenfunctions $\{Z_n(z,h,\eta), n = 0,1,2,3\ldots\}$.

(ii) On the basis of smoothness assumptions concerning the depth function $h(x)$ and the elevation $\eta(x,t)$, the series (4.1) can be term-by-term differentiated with respect to x, z, and t, leading to corresponding series expansions for the corresponding derivatives. For example,

$$\frac{\partial \varphi(x,z,t)}{\partial x} = \sum_{n=-2}^{\infty} \frac{\partial \varphi_n(x,t)}{\partial x} Z_n(z,h(x),\eta(x,t)) + \varphi_n(x,t)\frac{\partial Z_n(z,h(x),\eta(x,t))}{\partial x}, \tag{4.13a}$$

$$\frac{\partial \varphi(x,z,t)}{\partial z} = \sum_{n=-2}^{\infty} \varphi_n(x,t)\frac{\partial Z_n(z,h(x),\eta(x,t))}{\partial z}, \tag{4.13b}$$

$$\frac{\partial \varphi(x,z,t)}{\partial t} = \sum_{n=-2}^{\infty} \frac{\partial \varphi_n(x,t)}{\partial t} Z_n(z,h(x),\eta(x,t)) + \varphi_n(x,t)\frac{\partial Z_n(z,h(x),\eta(x,t))}{\partial t}. \tag{4.13c}$$

(iii) From Eqs. (4.8), we can clearly see that the sloping-bottom mode ($\varphi_{-1}Z_{-1}$) is zero, and thus it is not needed in subareas where the bottom is flat ($h'(x) = 0$). Moreover, the upper-surface mode ($\varphi_{-2}Z_{-2}$) becomes zero, and thus it is not needed only in the very special case of linearised (small-amplitude), monochromatic waves characterised by the frequency parameter $\mu = \omega^2/g$ that coincides with the numerical parameter μ_0 (i.e., $\mu = \mu_0$).

(iv) Finally, we note here that the series expansion (4.1) has been constructed bearing in mind its convergence properties and the smoothness requirements of the solution of the studied problem. None of the terms of the series (4.1) individually satisfies the differential (Laplace) equation and the boundary conditions of the problem. This is to be obtained by the sum of all terms, by the appropriate calculation of the mode amplitudes $\varphi_n(x,t), n = -2,-1,0,1,2,\ldots$, through the variational equation (3.2). The latter, as shown in the previous section, contains both the Laplace equation and the boundary conditions of the problem.

5. The coupled mode system of equations

The series expansion (4.1) permits us to obtain a series representation of the variation $\delta\varphi$ of the wave potential, in terms of the variations of the modal amplitudes φ_n and the upper surface elevation η. The general form of $\delta\varphi$ is given by

$$\delta\varphi(x,z,t) = \sum_{n=-2}^{\infty} \delta\varphi_n(x,t) Z_n(z,h,\eta) + \varphi_n(x,t)\delta Z_n(z,h,\eta). \tag{5.1}$$

Since $Z_n = Z_n(z,h,\eta)$ is independent of φ_n, we have, in general,

$$\delta Z_n(z,h,\eta) = W_n(z,h,\eta)\delta\eta, \quad \text{for } -h \le z < \eta, \tag{5.2a}$$

where

$$W_n(z,h,\eta) = \frac{\partial Z_n(z,h,\eta)}{\partial\eta}, \quad \text{for } -h \le z < \eta. \tag{5.2b}$$

The vertical modes $Z_n = Z_n(z,h,\eta)$, as given by Eqs. (4.2)–(4.4), are normalized, and on the upper surface, $z = \eta(x;t)$, they all take the constant value 1, i.e., $Z_n(z = \eta; h, \eta) = 1$. Thus, for points on the upper surface, it holds that $\delta Z_n = 0$.

Furthermore, the series expansion (4.1) of $\varphi(x,z,t)$ permits us to obtain corresponding modal series expansions for all expressions appearing in the right-hand side of Eqs. (3.3), as, for example, given by Eqs. (4.13) for the first spatial and time derivatives. Under the assumption that $\varphi_n(x,t)$ are twice continuously differentiable with respect to x, by introducing the above series in the variational equation (3.2) and using standard arguments of the calculus of variations, we eventually arrive at the following.

Theorem C. *The examined hydroelastic problem in the variable bathymetry region is equivalent to the* nonlinear Coupled-Mode System (CMS):

$$\frac{\partial\eta}{\partial t} + \sum_{n=-2}^{\infty}\left(A_{mn}(\eta)\frac{\partial^2\varphi_n}{\partial x^2} + B_{mn}(\eta)\frac{\partial\varphi_n}{\partial x} + C_{mn}(\eta)\varphi_n\right) = 0, \quad m = -2,-1,0,1,2\ldots, \tag{5.3a}$$

$$\chi\left(\frac{m}{\rho}\frac{\partial^2\eta}{\partial t^2} + \frac{D}{\rho}\frac{\partial^4\eta}{\partial x^4}\right) + g\eta + \sum_{n=-2}^{\infty}\left(\frac{\partial\varphi_n}{\partial t} + [W_n]_{z=\eta}\varphi_n\frac{\partial\eta}{\partial t}\right) - \sum_{\ell=-2}^{\infty}\sum_{n=-2}^{\infty}\left(a_{\ell n}^{(0,2)}(\eta)\varphi_\ell\frac{\partial^2\varphi_n}{\partial x^2} + a_{\ell n}^{(1,1)}(\eta)\frac{\partial\varphi_\ell}{\partial x}\frac{\partial\varphi_n}{\partial x} + b_{\ell n}(\eta)\varphi_\ell\frac{\partial\varphi_n}{\partial x} + c_{\ell n}(\eta)\varphi_\ell\varphi_n\right) = 0, \tag{5.3b}$$

for $-\infty < x < \infty$. In Eq. (5.3b), the function $\chi(x)$ is the characteristic function of the interval $a < x < b$ ($\chi = 1$, if $a < x < b$, and 0 otherwise). The CMS (5.3) is supplemented by the following edge conditions (cf. Eqs. (3.14) and (3.15)):

$$\frac{\partial^3\eta(x=a+0;t)}{\partial x^3} = 0 \quad \textit{and} \tag{5.4a}$$

$$\frac{\partial^3\eta(x=b-0;t)}{\partial x^3} = 0, \tag{5.4b}$$

$$\frac{\partial^2\eta(x=a+0;t)}{\partial x^2} = 0 \quad \textit{and} \tag{5.4c}$$

$$\frac{\partial^2\eta(x=b-0;t)}{\partial x^2} = 0. \tag{5.4d}$$

The matrix coefficients $A_{mn}(\eta)$, $B_{mn}(\eta)$, $C_{mn}(\eta)$, appearing in Eq. (5.3a), are dependent on the elevation η, and are expressed in terms of the local vertical modes $\{Z_n\}_{n=-2,-1,0,1,\ldots}$ and their derivatives, as follows:

$$A_{mn}(\eta) = \langle Z_n, Z_m\rangle = \int_{z=-h(x)}^{z=\eta(x;t)} Z_n(z,h,\eta)Z_m(z,h,\eta)\mathrm{d}z, \tag{5.5a}$$

$$B_{mn}(\eta) = 2\left\langle\frac{\partial Z_n}{\partial x}, Z_m\right\rangle + \frac{\partial h}{\partial x}[Z_nZ_m]_{z=-h} + \frac{\partial\eta}{\partial x}[Z_nZ_m]_{z=\eta}, \tag{5.5b}$$

$$C_{mn}(\eta) = \langle\Delta Z_n, Z_m\rangle + \left[\left(\frac{\partial h}{\partial x}\frac{\partial Z_n}{\partial x} + \frac{\partial Z_n}{\partial z}\right)Z_m\right]_{z=-h} + \left[\left(\frac{\partial\eta}{\partial x}\frac{\partial Z_n}{\partial x} - \frac{\partial Z_n}{\partial z}\right)Z_m\right]_{z=\eta}, \tag{5.5c}$$

where $\Delta Z_n = \frac{\partial^2 Z_n}{\partial x^2} + \frac{\partial^2 Z_n}{\partial z^2}$. The matrix coefficients $a_{mn}(\eta)$, $b_{mn}(\eta)$ and $c_{mn}(\eta)$, appearing in Eq. (5.3b), are also dependent on the elevation η, and are defined as follows:

$$a_{\ell n}^{(0,2)}(\eta) = \langle Z_n, W_\ell\rangle = \int_{z=-h(x)}^{z=\eta(x;t)} Z_n(z,h,\eta)W_\ell(z,h,\eta)\mathrm{d}z, \tag{5.6a}$$

$$a_{\ell n}^{(1,1)}(\eta) = -\frac{1}{2}[Z_nZ_\ell]_{z=\eta} = -\frac{1}{2}, \tag{5.6b}$$

$$b_{\ell n}(\eta) = 2\left\langle\frac{\partial Z_n}{\partial x}, W_\ell\right\rangle + \frac{\partial h}{\partial x}[Z_nW_\ell]_{z=-h} - \left[\frac{\partial Z_n}{\partial x}\right]_{z=\eta}, \tag{5.6c}$$

$$c_{\ell n}(\eta) = \langle\Delta Z_n, W_\ell\rangle + \left[\left(\frac{\partial h}{\partial x}\frac{\partial Z_n}{\partial x} + \frac{\partial Z_n}{\partial z}\right)W_\ell\right]_{z=-h} - \frac{1}{2}\left[\frac{\partial Z_\ell}{\partial x}\frac{\partial Z_n}{\partial x} + \frac{\partial Z_\ell}{\partial z}\frac{\partial Z_n}{\partial z}\right]_{z=\eta}. \tag{5.6d}$$

The nonlinear CMS, Eqs. (5.3) and (5.4), has been derived by the same variational principle, Eq. (3.2), and thus it is equivalent to the examined hydroelastic problem defined by Eqs. (3.11)–(3.15). Moreover, it has been obtained without any assumptions concerning the vertical structure of the wave potential. Thus, the present CMS, being equivalent to the complete formulation, is expected to be able to fully account for wave nonlinearity and dispersion.

Although the present CMS has been developed for the hydroelastic problem of the interaction of water waves with a large floating body (modelled as a thin elastic plate) in variable bathymetry regions, the hydrodynamic part of Eqs. (5.3), i.e. Eq. (5.3a) and ((5.3b), with $\chi = 0$), can also serve as a model for the propagation of nonlinear water waves in general bathymetry. In this context, the present CMS exhibits similarity to the fully dispersive, multiterm-coupling model by Nadaoka et al. [32]. As is the case with the latter model, a distinctive feature of the present CMS is that no simplifications have been introduced for its derivation. Thus, in principle, simplified models could be recovered as appropriate limiting forms of Eqs. ((5.3), with $\chi = 0$). For example, keeping only the propagating mode $Z_0(z)$ in the vertical expansion (4.1) and linearising the coupled-mode equations, the classical *mild-slope* model is obtained; see, e.g., Smith and Sprinks [36], Dingemans [10]. If the evanescent modes $Z_n(z)$, $n = 1, 2, \ldots$, are also retained, an *extended mild-slope* model is obtained; see, e.g., Massel [28]. If we keep only the quadratic vertical mode $Z_{-2}(z)$, defined by Eq. (4.2), in the vertical expansion of the wave potential and retain up to second-order terms in the present CMS, a *Boussinesq-type* model is obtained; see, e.g., Liu [25]. On the other hand, if we keep in the local-mode series only the propagating mode $Z_0(z) = \cosh(k_0(z+h))\cosh^{-1}(k_0(\eta+h))$ and again retain up to second-order terms, a two-equation, nonlinear, mild-slope model is derived, quite similar to the time-dependent, nonlinear, mild-slope equation by Beji and Nadaoka [5].

6. The weakly nonlinear CMS

A second-order, weakly nonlinear version of the present nonlinear CMS can be obtained by suppressing the explicit nonlinear terms appearing in Eqs. (5.3), (5.5) and (5.6) and retaining up to second-order contributions. To this end, we introduce the following expansion of the vertical local modes:

$$\begin{aligned} Z_n(z, h(x), \eta(x,t)) &= Z_n(z, h(x), \eta = 0) \\ &\quad + \eta(x,t) W_n(z, h(x), \eta = 0) + O(\eta^2), \\ &\quad n = -2, -1, 0, 1, 2, \ldots, \end{aligned} \tag{6.1}$$

where $W_n(z, h, \eta)$ has been defined by Eq. (5.2b). For convenience in the presentation, from now on we shall denote the functions $Z_n(z, h, \eta = 0)$ by $\tilde{Z}_n(z, h)$ and the functions $W_n(z, h, \eta = 0)$ by $\tilde{W}_n(z, h)$. Both families of functions are obtained from formulae (4.2)–(4.4), concerning Z_n, and Eq. (5.2b), concerning W_n, by setting $\eta = 0$. After carrying out the necessary algebra, we eventually arrive at the following second-order, *weakly nonlinear Coupled-Mode System* (in short *wnCMS*):

$$\begin{aligned} &\frac{\partial \eta}{\partial t} + \sum_{n=-2}^{\infty} \left(\tilde{A}_{mn} \frac{\partial^2 \varphi_n}{\partial x^2} + \tilde{B}_{mn} \frac{\partial \varphi_n}{\partial x} + \tilde{C}_{mn} \varphi_n \right) = 0, \\ &m = -2, -1, 0, 1, 2, \ldots, \end{aligned} \tag{6.2a}$$

and

$$\begin{aligned} &\chi \left(\frac{m}{\rho} \frac{\partial^2 \eta}{\partial t^2} + \frac{D}{\rho} \frac{\partial^4 \eta}{\partial x^4} \right) + g\eta + \sum_{n=-2}^{\infty} \left(\frac{\partial \varphi_n}{\partial t} + \tilde{w}_n \varphi_n \frac{\partial \eta}{\partial t} \right) \\ &- \sum_{\ell=-2}^{\infty} \sum_{n=-2}^{\infty} \left(\tilde{a}_{\ell n}^{(0,2)} \varphi_\ell \frac{\partial^2 \varphi_n}{\partial x^2} + \tilde{a}_{\ell n}^{(1,1)} \frac{\partial \varphi_\ell}{\partial x} \frac{\partial \varphi_n}{\partial x} \right. \\ &\left. + \tilde{b}_{\ell n} \varphi_\ell \frac{\partial \varphi_n}{\partial x} + \tilde{c}_{\ell n} \varphi_\ell \varphi_n \right) = 0 \end{aligned} \tag{6.2b}$$

for $-\infty < x < \infty$. The wnCMS (6.2) is also supplemented by the same plate edge conditions, Eqs. (5.4).

In the present case, the coefficients $\tilde{A}_{mn}$, $\tilde{B}_{mn}$ and $\tilde{C}_{mn}$ are obtained from Eqs. (5.5) and (5.6), using the approximation (6.1) as follows:

$$\tilde{A}_{mn} = \tilde{A}_{mn}^{(0)} + \eta \tilde{A}_{mn}^{(1)} + O(\eta^2), \tag{6.3a}$$

$$\tilde{B}_{mn} = \tilde{B}_{mn}^{(0)} + \eta \tilde{B}_{mn}^{(1)} + \frac{\partial \eta}{\partial x} \tilde{B}_{mn}^{(2)} + O(\eta^2), \tag{6.3b}$$

$$\tilde{C}_{mn} = \tilde{C}_{mn}^{(0)} + \eta \tilde{C}_{mn}^{(1)} + \frac{\partial \eta}{\partial x} \tilde{C}_{mn}^{(2)} + \frac{\partial^2 \eta}{\partial x^2} \tilde{C}_{mn}^{(3)} + O(\eta^2), \tag{6.3c}$$

and thus they become explicitly dependent on the upper-boundary elevation $\eta(x,t)$.

The coefficients $\tilde{A}_{mn}^{(0,1)}$, $\tilde{B}_{mn}^{(0,1,2)}$ and $\tilde{C}_{mn}^{(0,1,2,3)}$ involved in Eqs. (6.3), and the coefficients $\tilde{w}_n$, $\tilde{a}_{\ell n}^{(0,2)}$, $\tilde{a}_{\ell n}^{(1,1)}$, $\tilde{b}_{\ell n}$ and $\tilde{c}_{\ell n}$ involved in Eq. (6.2b), are all time-independent quantities. These are defined in terms of the local vertical modes $\{\tilde{Z}_n(z,h)\}_{n=-2,-1,0,1,\ldots}$ in the interval $-h(x) \le z \le 0$ and their derivatives, and they are listed in the Appendix.

Two crucial facts concerning the theoretical value and practical effectiveness of the second-order wnCMS, Eqs. (6.2), are the following. (i) A small number of modes, e.g., 5 to 6, is practically enough for numerical convergence, even in cases of very steep bathymetry. Extensive numerical evidence suggests that the mode amplitudes exhibit a fast rate of decay, which ensures fast algebraic convergence of the modal series (4.1). (ii) The first three modes in the series, i.e., the newly introduced upper-surface mode $\varphi_{-2}(x,t)$ and sloping-bottom mode $\varphi_{-1}(x,t)$, and the propagating mode $\varphi_0(x;t)$, are the most important terms in the series expansion, being one order of magnitude higher than the other modes $\varphi_n(x,t)$, $n = 1, 2, 3, \ldots$.

The above facts will also be confirmed by examining the linearised dispersion characteristics of the present coupled mode system, described in the next section.

7. Dispersion characteristics of the present CMS

To study the dispersion characteristics of the present coupled-mode system in constant depth, we first proceed to its linearisation. This is obtained by suppressing all nonlinearities appearing in Eqs. (6.2). In this case, the coupled-mode system reduces to its linear version, composed of the equations

$$\frac{\partial\eta}{\partial t}+\sum_{n=-2}^{\infty}\left(\tilde{A}^{(0)}_{mn}\frac{\partial^2\varphi_n}{\partial x^2}+\tilde{B}^{(0)}_{mn}\frac{\partial\varphi_n}{\partial x}+\tilde{C}^{(0)}_{mn}\varphi_n\right)=0,$$
$$m=-2,-1,0,1,2,\ldots, \tag{7.1a}$$

and

$$\chi\left(\frac{m}{\rho}\frac{\partial^2\eta}{\partial t^2}+\frac{D}{\rho}\frac{\partial^4\eta}{\partial x^4}\right)+g\eta+\sum_{n=-2}^{\infty}\frac{\partial\varphi_n}{\partial t}=0. \tag{7.1b}$$

The coefficients $\tilde{A}^{(0)}_{mn}$, $\tilde{B}^{(0)}_{mn}$ and $\tilde{C}^{(0)}_{mn}$ of the linearised system, appearing in Eq. (7.1a), are all independent of the elevation η. These coefficients, given by Eqs. (A.1a), (A.2a) and (A.3a) in the Appendix, are dependent only on the horizontal coordinate x, through the local depth function $h(x)$.

By differentiating Eq. (7.1b) once with respect to time and substituting into (7.1a), we obtain

$$\sum_{n=-2}^{\infty}\left(-\frac{1}{g}\frac{\partial^2\varphi_n}{\partial t^2}+\tilde{A}^{(0)}_{mn}\frac{\partial^2\varphi_n}{\partial x^2}+\tilde{B}^{(0)}_{mn}\frac{\partial\varphi_n}{\partial x}+\tilde{C}^{(0)}_{mn}\varphi_n\right)$$
$$=\chi\left(\varepsilon\frac{\partial^3\eta}{\partial t^3}+\delta\frac{\partial^4}{\partial x^4}\frac{\partial\eta}{\partial t}\right),$$
$$m=-2,-1,0,1,2,\ldots, \tag{7.2a}$$

and

$$\chi\left(\varepsilon\frac{\partial^2\eta}{\partial t^2}+\delta\frac{\partial^4\eta}{\partial x^4}\right)+\eta+\frac{1}{g}\sum_{n=-2}^{\infty}\frac{\partial\varphi_n}{\partial t}=0, \tag{7.2b}$$

where $\varepsilon=m/\rho g$ and $\delta=D/\rho g=EI/\rho g$. Restricting ourselves to the constant-depth case, the sloping-bottom mode $\varphi_{-1}(x,t)$ becomes identically zero (cf. Eqs. (4.7) and (4.8b)), as well as the coefficients $\tilde{B}^{(0)}_{mn}=0$ (see Eq. (A.2a)). Also, in this case, the coefficients $\tilde{A}^{(0)}_{mn}$ and $\tilde{C}^{(0)}_{mn}$ take constant values for all x.

7.1. Water waves under the free-surface

We first examine the case of water waves, without the presence of the elastic plate, in constant depth. On the basis of Eq. (7.2a), using $\chi=0$ and $\tilde{B}^{(0)}_{mn}=0$, the time-domain linearised coupled-mode system reduces to

$$\sum_{\substack{n=-2\\n\neq-1}}^{M}\left(-\frac{\partial^2\varphi_n}{\partial t^2}+\alpha_{mn}\frac{\partial^2\varphi_n}{\partial x^2}+\gamma_{mn}\varphi_n\right)=0,$$
$$m=-2,0,1,2,\ldots, \tag{7.3}$$

where the coefficients $\alpha_{mn}=g\tilde{A}^{(0)}_{mn}$ and $\gamma_{mn}=g\tilde{C}^{(0)}_{mn}$ are dependent only on h and the numerical parameters μ_0 and h_0. In order to investigate the dispersion characteristics of the coupled-mode system in this case, we examine if it admits simple harmonic solutions of the form

$$\varphi_n(x,t)=f_n\cos(k(x\mp\hat{C}t)),\quad n=-2,0,1,2,\ldots, \tag{7.4}$$

and find out the dependence (in non-dimensional form) of the quantity

$$\frac{\hat{C}}{\sqrt{gh}}=\hat{\mathsf{C}}(kh), \tag{7.5a}$$

from the non-dimensional wavenumber kh. In the above equations, $\hat{C}$ denotes the phase speed of the harmonic solution (7.4), h is the (constant) depth considered, and f_n are the amplitudes of the modes. We recall from linearised water-wave theory, that the exact form of the dispersion relation is

$$\frac{C}{\sqrt{gh}}=\mathsf{C}(kh)=\sqrt{\frac{\tanh(kh)}{kh}}. \tag{7.5b}$$

By introducing the representations (7.4) to the linearised coupled-mode system (7.3) we obtain the following algebraic system

$$\sum_{\substack{n=-2\\n\neq-1}}^{M}(-k^2\alpha_{mn}+(\gamma_{mn}+k^2\hat{C}^2))f_n=0,$$
$$m=-2,0,1,2,\ldots. \tag{7.6}$$

Non-trivial solutions of the homogeneous system (7.6) are obtained by requiring its determinant to vanish, which can then be used for calculating $\hat{\mathsf{C}}(kh)$ and comparing with the analytical result, Eq. (7.5b). Fig. 3 presents such a comparison, obtained by using $\mu_0 h=0.25$ and $\mu_0 h_0=1$, and by keeping 1 term (only mode 0), 3 terms (modes −2,0,1) and 5 terms (modes −2,0,1,2,3) in the local-mode series. Recall that, in this case, the bottom is flat and thus the sloping-bottom mode (mode −1) is zero by definition and does not need to be included. On the other hand, the inclusion of the additional upper-surface mode (mode −2) in the local-mode series substantially improves its convergence to the exact result, for an extended range of wave frequencies, ranging from shallow to deep water-wave conditions. In the example shown in Fig. 3 using 5 terms (thick dashed line), the error is less than 1%, for kh up to 10, and less than 5%, for kh up to 16. However, we wish to note here that, if mode 0 (propagating mode) is included in the modal series (which is suggested), the dispersion characteristics of the present approximation (even using only 1 term) matches the analytical curve at the point k_*h, where $k_*h\tanh k_*h=\mu_0 h$, indicated by using a vertical arrow in Fig. 3.

Consequently, by appropriate choice of the numerical parameter μ_0, we are able to obtain a good approximation for kh lying in an interval around the point k_*h, even when the number of terms retained in the modal series is small. Moreover, extensive numerical investigation of the effects of the numerical parameters μ_0 and h_0 on the dispersion characteristics of the present CMS has revealed that, if the number of modes retained in the local-mode series is equal or greater than 6, the results become practically independent (error less than 0.5%) from the specific choice for the values of the (numerical) parameters μ_0 and h_0, for all non-dimensional wavenumbers in the interval $0<kh<24$.

Quite similar results are obtained concerning the vertical distribution of the wave potential and velocity. In conclusion,

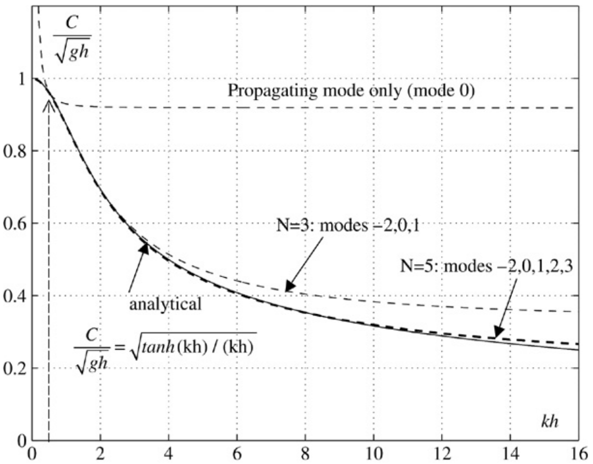

Fig. 3. Dispersion characteristics of the present coupled mode system using the local-mode representation (4.1), keeping 1 and 3 terms (dashed lines) and 5 terms (thick dashed line) in the series. The values of the numerical parameters used are: $\mu_0 h = 0.25$ and $\mu_0 h_0 = 1$. The analytical result is shown by a solid line.

a few modes (of the order of 5 to 6) are sufficient for modelling fully dispersive waves in a constant-depth strip, for an extended range of frequencies. In the more general case of variable bathymetry regions, the enhancement of the local-mode series (4.1) by the inclusion of the sloping-bottom mode ($n = -1$) in the representation of the wave potential is of utmost importance concerning consistent satisfaction of the Neumann boundary condition (necessitating zero normal velocity) on the sloping parts of the bottom. This requirement has been discussed in detail in [2] and in [8], where it is also shown that the enhanced series exhibits improved convergence due to the fast rate of decay of the modal amplitudes $|\varphi_n(x)| \approx O(n^{-4})$. Thus, a small number of modes suffices to obtain a convergent solution to $\varphi(x, z, t)$, for bottom slopes of the order of 1, or even higher.

7.2. *Water waves under the elastic-plate surface*

Working similarly, as in the previous subsection, we examine the linearised coupled-mode system, in constant depth, under the elastic plate, as defined by Eq. (7.2), using $\chi = 1$ and $\tilde{B}_{mn}^{(0)} = 0$,

$$\sum_{\substack{n=-2\\n\neq-1}}^{M} \left(-\frac{\partial^2 \varphi_n}{\partial t^2} + \alpha_{mn} \frac{\partial^2 \varphi_n}{\partial x^2} + \gamma_{mn} \varphi_n \right) = g \left(\varepsilon \frac{\partial^3 \eta}{\partial t^3} + \delta \frac{\partial^4}{\partial x^4} \frac{\partial \eta}{\partial t} \right), \quad m = -2, 0, 1, 2, \ldots, \tag{7.7a}$$

$$\left(\varepsilon \frac{\partial^2 \eta}{\partial t^2} + \delta \frac{\partial^4 \eta}{\partial x^4} \right) + \eta + \frac{1}{g} \sum_{\substack{n=-2\\n\neq-1}}^{M} \frac{\partial \varphi_n}{\partial t} = 0, \tag{7.7b}$$

where the coefficients α_{mn} and γ_{mn} are the same as before ($\alpha_{mn} = g\tilde{A}_{mn}^{(0)}$ and $\gamma_{mn} = g\tilde{C}_{mn}^{(0)}$). In this case, we seek simple harmonic solutions of Eq. (7.7) of the form

$$\varphi_n(x, t) = f_n \cos(k_E(x \mp \hat{C}_E t)), \quad n = -2, 0, 1, 2, \ldots,$$
$$\eta(x, t) = \beta \sin(k_E(x \mp \hat{C}_E t)), \tag{7.8}$$

where β denotes the amplitude of the elastic-plate deflection. Using Eq. (7.7b) to eliminate β through the mode amplitudes f_n, and substituting to Eq. (7.7a), we eventually arrive at the following homogeneous system:

$$\sum_{\substack{n=-2\\n\neq-1}}^{M} \left(-k_E^2 \alpha_{mn} + \gamma_{mn} + \frac{k_E^2 \hat{C}_E^2}{\delta k_E^4 - \varepsilon k_E^2 \hat{C}_E^2 + 1} \right) f_n = 0, \quad m = -2, 0, 1, 2, \ldots. \tag{7.9}$$

Non-trivial solutions of the system (7.9) are again obtained by requiring its determinant to vanish, which can be used for calculating the phase speed $\hat{C}_E = \hat{C}_E(k_E h)$ of the waves below the elastic plate and compare with the analytical result, which in this case is

$$\frac{C_E}{\sqrt{gh}} = C_E(k_E h) = \frac{1}{k_E} \sqrt{\frac{\mu}{h}}, \tag{7.10a}$$

where k_E is the positive real root of the elastic-plate dispersion relation [22,38,1],

$$\mu = (\delta k_E^4 + 1 - \varepsilon) k_E \tanh(k_E h). \tag{7.10b}$$

Fig. 4 presents such a comparison for an elastic plate with parameters $\delta = 10^5$ m^4 per meter in the transverse (y) direction and $\varepsilon = 0$ (which is a usual approximation). Numerical results have being obtained by using the same values of the numerical parameters as before ($\mu_0 h = 0.25$ and $\mu_0 h_0 = 1$) and by keeping 1 term (only mode 0), 3 terms (modes −2,0,1) and 5 terms (modes −2,0,1,2,3) in the local-mode series (4.1) and in the system (7.9). The results shown in Fig. 4, for $N = 3$ and 5, have been obtained by including the upper-surface mode ($n = -2$) in the local-mode series representation (4.1). We recall here that, in the case examined (constant-depth strip), the bottom is flat, and thus the sloping-bottom mode ($n = -1$) is zero (by definition) and does not need to be included.

Once again, the fast convergence of the present method to the exact (analytical) solution, given by Eqs. (7.10), is clearly illustrated. Also, in this case, extensive numerical evidence has revealed that, if the number of modes retained in the local-mode series is greater than 6, the results remain practically independent from the specific choice of the (numerical) parameters μ_0 and h_0, and the dispersion curve $\hat{C}_E(kh)$ agrees very well with the analytical one, for non-dimensional wavenumbers in the interval $0 < k_E h < 24$, corresponding to an extended band of frequencies.

8. Numerical examples

The discrete version of the wnCMS (6.2) is obtained by truncating the local-mode series (4.1) to a finite number of terms (modes), and using second-order finite differences, based on time step Δt, to approximate the time derivatives appearing in the system. Also, an 1/4-1/2-1/4 discrete scheme (defined at $t - \Delta t$, t, $t + \Delta t$) using central, second-order spatial finite differences, based on a step Δx, is used to approximate the horizontal derivatives in the system. Discrete boundary conditions are obtained by using second-order forward and

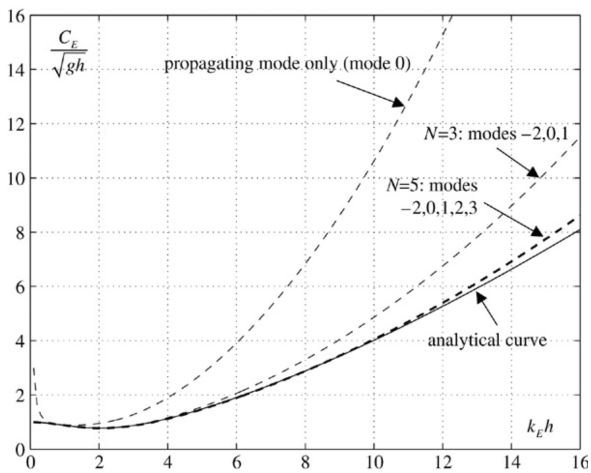

Fig. 4. Dispersion characteristics of the present coupled-mode system for waves in a constant-depth strip under a floating elastic plate, using the enhanced local-mode representation (4.1), and retaining 1 and 3 terms (dashed lines) and 5 terms (thick dashed line) terms. Elastic plate parameters are $\delta = 10^5$ m^4 per meter in the transverse (y) direction and $\varepsilon = 0$. The values of the (numerical) parameters used in the calculations are: $\mu_0 h = 0.25$ and $\mu_0 h_0 = 1$. The analytical result is shown by a solid line.

backward differences to approximate the horizontal derivatives in the boundary conditions, Eqs. (5.4), at $x = a$ and $x = b$. Thus, the discrete scheme is a fully implicit finite difference scheme, uniformly of second order in the horizontal (spatial) dimension. Numerical experience has shown that the stability of the present discrete scheme is controlled by a Courant number $C\Delta t/\Delta x$ (where C is a representative value of the waves phase speed in the domain D), which must take values much lower than unity.

In this section, we concern ourselves with the derivation and presentation of numerical results in the simpler case of monochromatic waves, leaving the more interesting and complex problem of the propagation of multichromatic waves and wavepackets in variable bathymetry regions to be the subject of a future work.

8.1. Monochromatic Stokes waves in constant depth and in variable bathymetry

To demonstrate the applicability of our weakly nonlinear model, in this section we first present two particular examples, dealing with monochromatic waves propagating in constant depth and above a smooth but very steep shoal. In the first case, the present model results are compared with the results of the standard second-order Stokes theory; see, e.g., [10]. In the case of variable bathymetry, the present model results are compared with the frequency-domain solution, corresponding to the extension of Stokes theory in variable bathymetry, developed by Belibassakis and Athanassoulis [6]. In both examples, a total number of 6 modes ($n = -2, -1, 0, 1, 2, 3$) have been retained in the enhanced local-mode series (4.1).

In the first example, we consider harmonic incident waves of period $T = 5.7$ s and height $H = 2$ m propagating in constant depth $h = 6$ m. In this case, the wavelength-to-depth ratio is $\lambda/h = 6.4$ and the waveheight-to-depth ratio is $H/h = 0.34$, both parameters falling well inside the Stokes waves regime. Numerical results obtained using the present model are shown in Fig. 5. Starting from rest, the calculated wave field converges to the analytical second-order Stokes solution (Dingemans [10]) after about 15 periods. The latter is shown in the last frame of Fig. 5 using crosses.

As a second example, we consider harmonic incident waves of period $T = 3$ s and height $H = 0.6$ m, propagating over a smooth but very steep shoal, connecting two half-strips of constant but different depth. The bottom profile is characterised by the following depth function:

$$h(x) = \frac{h_1 + h_3}{2} - \frac{h_1 - h_3}{2} \tanh\left(3\pi\left(\frac{x-a}{b-a} - \frac{1}{2}\right)\right), \quad a < x < b. \tag{8.1}$$

where $h_1 = 6$ m for $x < a = 20$ m, and $h_3 = 2$ m for $x > b = 40$ m. The maximum bottom slope of this underwater shoal is 95%, and the mean bottom slope is 20%.

In this case, the wavelength-to-depth ratio λ/h varies from 2.3 to 5.5 and the waveheight-to-depth ratio H/h varies from 0.1 to 0.3, both parameters falling again within the Stokes waves regime. Numerical results obtained using the present model are shown in Fig. 6. Starting from rest, the calculated wave field converges to the time-harmonic solution after about 10–15 periods. A comparison is presented in the last frame of Fig. 5, between the present time-domain solution and the frequency-domain Stokes solution in variable bathymetry [6] indicated using crosses. In this case, the effects of weakly nonlinear, second-harmonic generation are evident, especially as the shallow end of the shoal is approached. This is illustrated in the last frames of Fig. 5, where we are able to observe the wavelength variation and the increase in the wave amplitude due to shoaling, as well as the fact that the waveform changes from sinusoidal to second-order Stokes form. It is also interesting to note here that, in the previous examples (and in many other cases examined by the authors), the rate of decay of modal amplitudes φ_n is found (numerically) to exhibit a very rapid decay:

$$\max_{a<x<b} |\varphi_n| = O(n^{-4}), \tag{8.2}$$

ensuring the fast algebraic convergence of the present local-mode series. Similar calculations carried out without including the two additional modes (upper-surface mode and sloping-bottom mode) in the representation of the wave potential, i.e., keeping only the modes $\varphi_0, \varphi_1, \varphi_2, \ldots$, revealed that the rate of decay of the modal amplitudes is much slower, $\max|\varphi_n| = O(n^{-2})$, fully justifying the inclusion of the two additional modes (φ_{-2} and φ_{-1}) in the present local-mode series expansion.

8.2. Scattering of monochromatic waves by an elastic plate in variable bathymetry

As a final example, in Figs. 7 and 8 we examine the hydroelastic behaviour of a thin elastic plate floating over a smooth

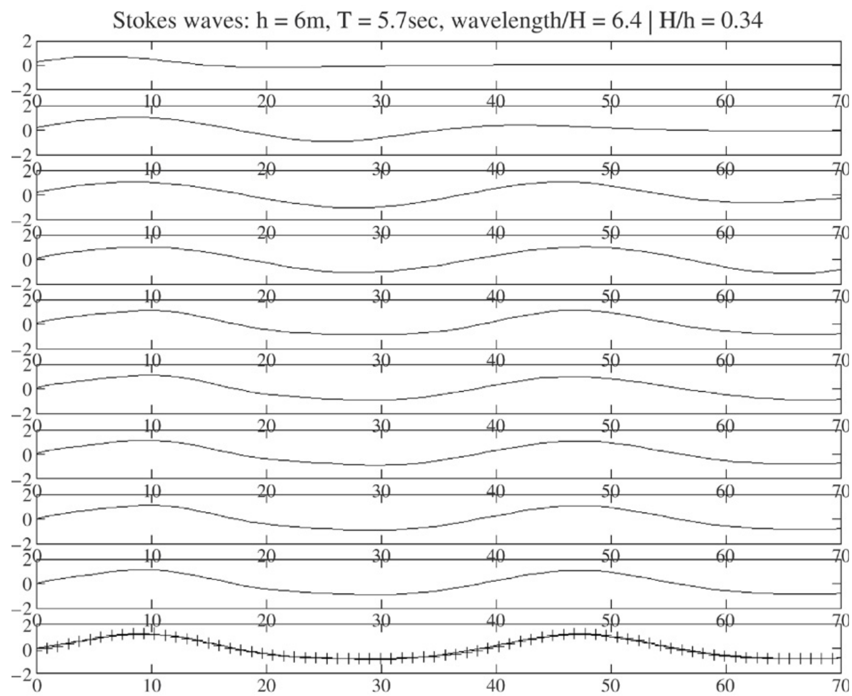

Fig. 5. Application of wnCMS to harmonic waves propagating in a constant-depth strip ($h = 6$ m). The period of the incoming waves is $T = 5.7$ s. The frames, from top to the bottom, show snapshots of the free-surface elevation, at equal time intervals $\delta t = 2T = 11.4$ s. The classical, time-harmonic, second-order Stokes solution has also been plotted in the last frame using crosses.

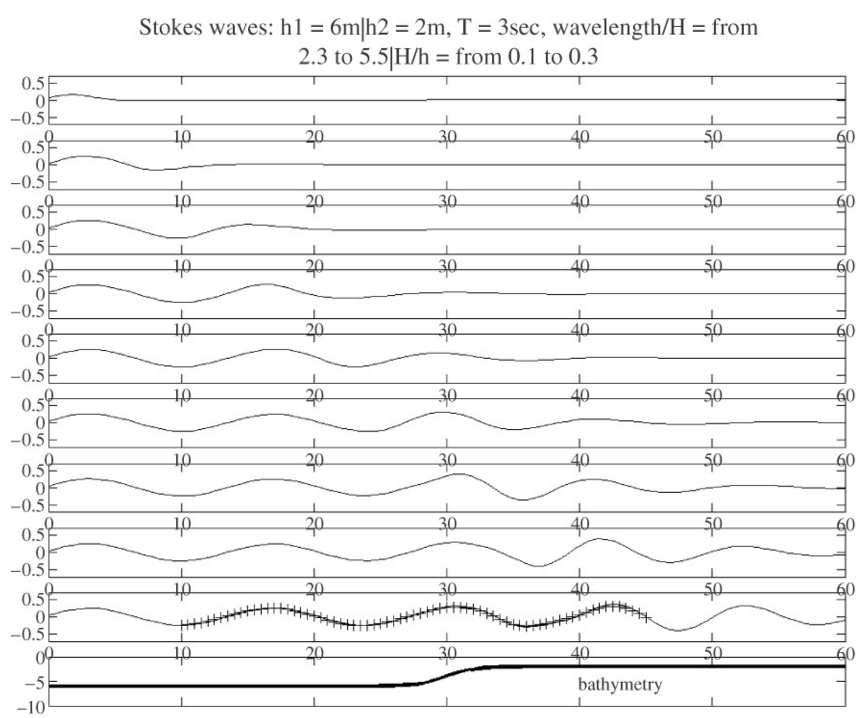

Fig. 6. Evolution of incident harmonic waves over a smooth but very steep shoal. The period of the incoming waves is $T = 3$ s. The frames, from top to the bottom, show the free-surface elevation obtained from the direct numerical solution of the wnCMS, at equal time intervals $\delta t = T = 3$ s. The monochromatic second-order Stokes solution in variable bathymetry [6] has also been plotted in the last frame using crosses.

shoal, modelling a VLFS. The depth profile (shown in the last subplot of Fig. 7) is taken to be given by the same Eq. (8.1), using $h_1 = 15$ m, $h_3 = 5$ m, and $a = 250$ m, $b = 750$ m. The average and maximum values of the slope of this bottom profile are 2% and 9.5%, respectively. The elastic plate is taken to extend from $x = a = 250$ m to $x = b = 750$ m, and thus, its

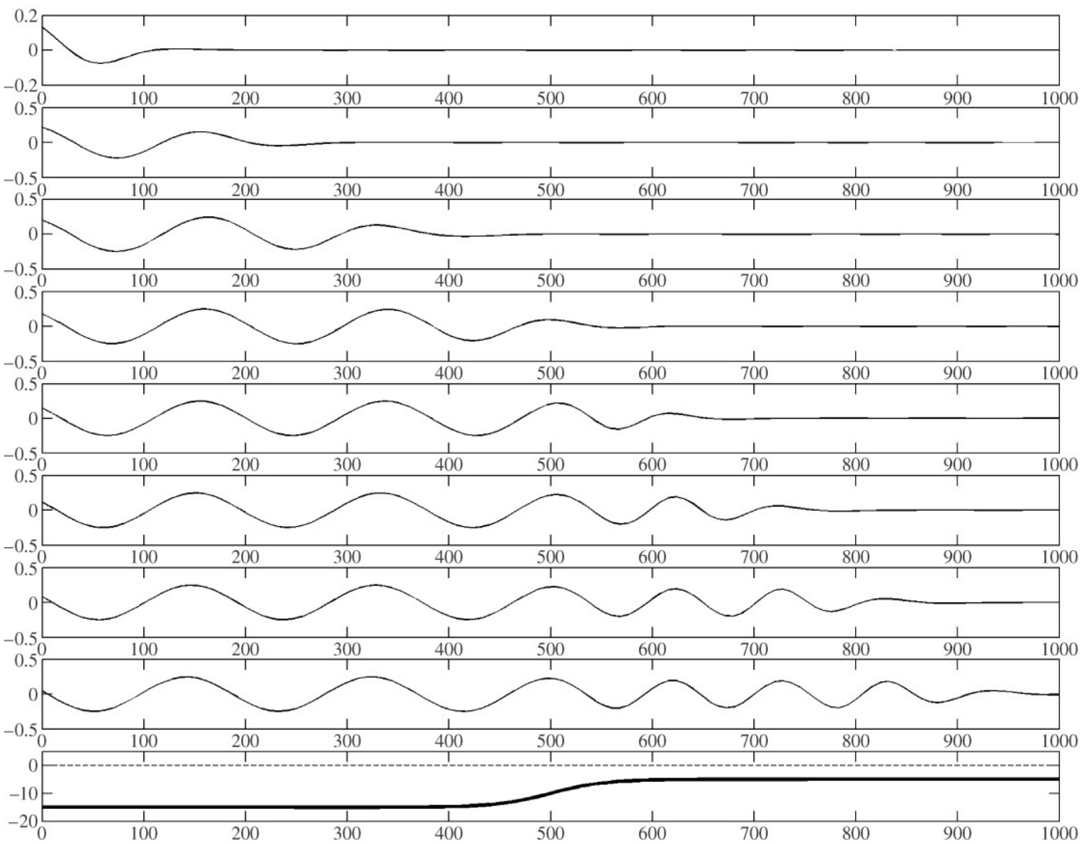

Fig. 7. Evolution of incident harmonic waves over a smooth shoal. The bathymetry is defined by Eq. (8.1) with $a = 250$ m and $b = 750$ m. The period of the incoming waves is $T = 15.7$ s ($\omega = 0.4$ rad/s). The frames, from top to the bottom, show the spatial evolution of the free-surface elevation, as obtained by the present wnCMS, at equal time intervals $\delta t = T$.

width is $L = b - a = 500$ m. The flexural rigidity parameter of the plate is $\delta = 10^5$ m^4 (per meter in the y-direction), and, for simplicity, the mass parameter is taken to be $\varepsilon = 0$, which is a usual assumption concerning VLFS applications.

The angular frequency of the incident wave has been selected to be $\omega = 0.4$ rad/s, and thus the wave conditions lie in the borderline between intermediate and shallow water depth. Also, the waveheight of the incident wave is taken to be $H = 0.25$ m, and thus the wave non-linearity remains at relatively low levels.

In order to examine the effects of the floating elastic plate on the diffraction of water waves, in Fig. 7 we first examine the evolution of incident harmonic waves over the smooth shoal, without the presence of the floating plate. The frames, from the top to the bottom, show the spatial evolution of the free-surface elevation, as obtained by the present wnCMS, at equal time intervals $\delta t = T = 15.7$ s. Again, we can clearly observe the continuous wavelength variation and the increase in the wave amplitude due to shoaling.

In Fig. 8, the large-time form of the upper surface elevation is shown with and without considering the effects of the floating elastic plate, as obtained by the present wnCMS. The frames, from top to the bottom, show the calculated elevation $\eta(x, t)$, at equal time intervals within one period. The free-surface elevation is plotted by thin solid lines and the elastic plate deflection by thick solid lines, respectively. For comparison, the free-surface elevation over the same variable bathymetry region, at the same instances, without taking into account the scattering effect by the elastic plate, has been overplotted in Fig. 8 using dashed lines.

We can observe in Fig. 8 that the presence of the elastic plate significantly modifies the wavelength in the variable bathymetry region. Moreover, the elastic plate deflection at the plate ends increases in comparison to the free-surface elevation in the same region, as obtained without consideration of the floating elastic plate. The deflection may become significant, especially at the downwave end of the plate, where the amplitude of transmitted wave could also increase. This result is justified by the higher hydroelastic excitation of waves in the fluid domain under the elastic plate, induced by the diffracted wave energy from the shoal. Future work is directed towards the systematic examination of combined scattering effects by the seabed and the elastic floating plate, both for shoaling and undulating bottom profiles, aiming to quantify the effects of general seabed topography (bottom slope and curvature) on the hydroelastic responses of the system.

9. Conclusions

The scattering problem of weakly nonlinear gravity waves by a large floating elastic structure over a general

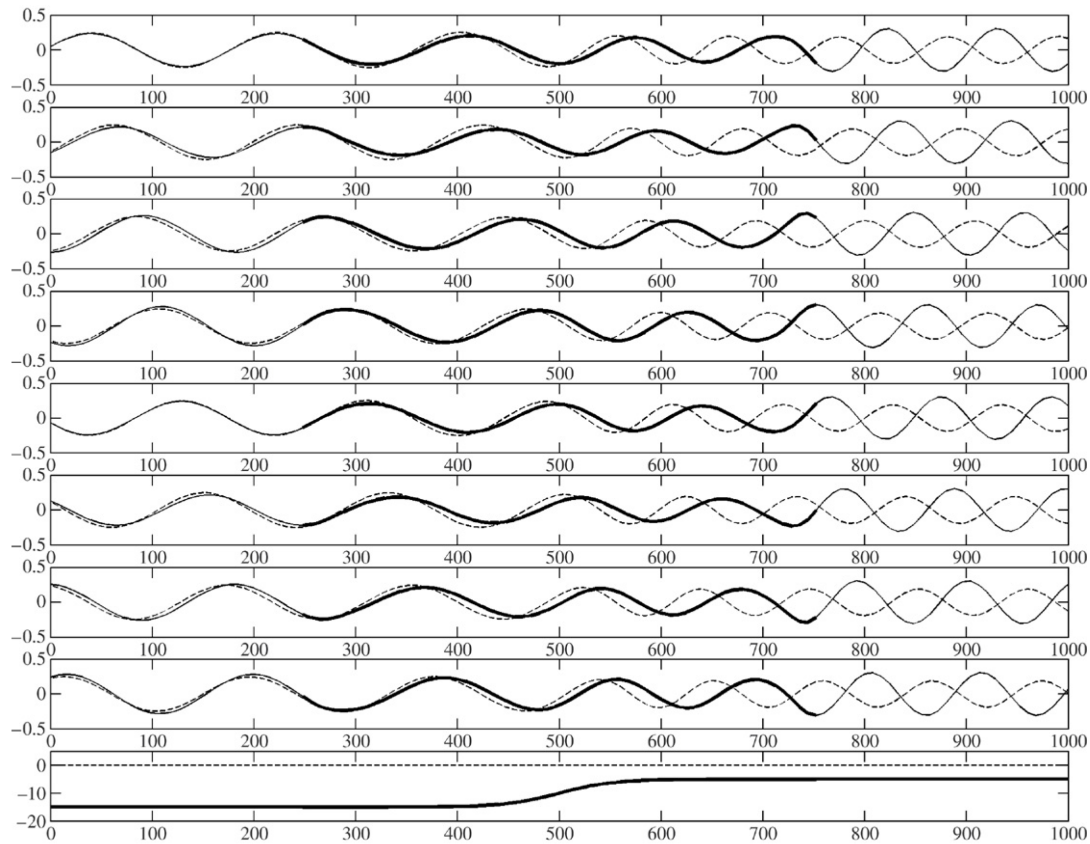

Fig. 8. Diffraction of incident harmonic waves by a floating elastic plate, with parameters $L = 500$ m, $\delta = 10^5$ m^4, $\varepsilon = 0$, lying over a smooth shoal, extending from $x = 250$ m to $x = 750$ m. The bathymetry and the period of the incoming waves are the same as in Fig. 7. The frames, from top to the bottom, show the large-time form of the upper-surface elevation, as obtained by the present wnCMS, at equal time intervals within one period. The free-surface elevation is shown by thin solid lines and the elastic plate deflection by thick solid lines, respectively. For comparison, the free-surface elevation at the same instances without the elastic plate is also plotted by dashed lines.

bathymetry is considered. An appropriate generalisation of Luke's variational principle [26] is derived, which models the evolution of nonlinear water waves in variable bathymetry regions, including the scattering effects by a thin floating elastic plate. A complete local-mode series expansion of the wave potential has been developed, which, used in the variational principle, enables us to reformulate the original problem as an infinite, coupled-mode system of nonlinear equations in the propagation (horizontal) space, with respect to the mode amplitudes, the free-surface elevation, and the elastic plate deflection. By keeping up to second-order nonlinearities, a weakly nonlinear coupled-mode system has been derived which fully accounts for the effects of weak nonlinearity and dispersion, applicable both to deep water and to intermediate water depth.

A specific feature of the present approach is that the local-mode series converges very fast, and thus only a small number of modes (up to 5 or 6) is practically enough for an accurate numerical solution, provided that the two new modes (the upper-surface mode and the sloping-bottom mode) are included in the local-mode series.

Finally, important aspects of the present method are that it can be extended further to treat fully three-dimensional problems, as well as large floating elastic bodies or structures characterised by variable thickness (draft), flexural rigidity, and mass distributions.

Appendix. Coefficients of the second-order coupled-mode system (wnCMS)

The coefficients $\tilde{A}_{mn}^{(0,1)}$, $\tilde{B}_{mn}^{(0,1,2)}$, $\tilde{C}_{mn}^{(0,1,2,3)}$ of the second-order Coupled-Mode System (wnCMS), Eq. (6.3), are given by

$$\tilde{A}_{mn}^{(0)} = \langle \tilde{Z}_n, \tilde{Z}_m \rangle_0 = \int_{z=-h(x)}^{z=0} \tilde{Z}_n(z,h)\tilde{Z}_m(z,h)\mathrm{d}z, \tag{A.1a}$$

$$\tilde{A}_{mn}^{(1)} = 1 + \langle \tilde{W}_n, \tilde{Z}_m \rangle_0 + \langle \tilde{Z}_n, \tilde{W}_m \rangle_0, \tag{A.1b}$$

$$\tilde{B}_{mn}^{(0)} = 2\left\langle \frac{\partial \tilde{Z}_n}{\partial x}, \tilde{Z}_m \right\rangle_0 + \frac{\partial h}{\partial x}[\tilde{Z}_n \tilde{Z}_m]_{z=-h}, \tag{A.2a}$$

$$\tilde{B}_{mn}^{(1)} = 2\left\langle \frac{\partial \tilde{W}_n}{\partial x}, \tilde{Z}_m \right\rangle_0 + 2\left\langle \frac{\partial \tilde{Z}_n}{\partial x}, \tilde{W}_m \right\rangle_0 + 2\left[\frac{\partial \tilde{Z}_n}{\partial x}\right]_{z=0} + \frac{\partial h}{\partial x}\left[\tilde{Z}_n \tilde{W}_m + \tilde{W}_n \tilde{Z}_m\right]_{z=-h}, \tag{A.2b}$$

$$\tilde{B}_{mn}^{(2)} = 2\langle \tilde{W}_n, \tilde{Z}_m \rangle_0 + 1, \tag{A.2c}$$

$$\tilde{C}_{mn}^{(0)} = \langle \Delta \tilde{Z}_n, \tilde{Z}_m \rangle_0 + \left[\left(\frac{\partial h}{\partial x} \frac{\partial \tilde{Z}_n}{\partial x} + \frac{\partial \tilde{Z}_n}{\partial z} \right) \tilde{Z}_m \right]_{z=-h} - \left[\frac{\partial \tilde{Z}_n}{\partial z} \right]_{z=0}, \tag{A.3a}$$

$$\tilde{C}_{mn}^{(1)} = \langle \Delta \tilde{Z}_n, \tilde{W}_m \rangle_0 + \langle \Delta \tilde{W}_n, \tilde{Z}_m \rangle_0 + \left[\Delta \tilde{Z}_n \right]_{z=0} + \frac{\partial h}{\partial x} \left[\left(\frac{\partial \tilde{Z}_n}{\partial x} \tilde{W}_m + \frac{\partial \tilde{W}_n}{\partial x} \tilde{Z}_m \right) \right]_{z=-h} + \left[\left(\frac{\partial \tilde{Z}_n}{\partial z} \tilde{W}_m + \frac{\partial \tilde{W}_n}{\partial z} \tilde{Z}_m \right) \right]_{z=-h}, \tag{A.3b}$$

$$\tilde{C}_{mn}^{(2)} = \left\langle \frac{\partial \tilde{W}_n}{\partial x}, \tilde{Z}_m \right\rangle_0 + \frac{\partial h}{\partial x} \left[\tilde{W}_n \tilde{Z}_m \right]_{-h} + \left[\frac{\partial \tilde{Z}_n}{\partial x} \right]_{z=0}, \tag{A.3c}$$

$$\tilde{C}_{mn}^{(3)} = \langle \tilde{Z}_m, \tilde{W}_n \rangle_0. \tag{A.3d}$$

Furthermore, the coefficients $\tilde{w}_n$, $\tilde{a}_{\ell n}^{(0,2)}$, $\tilde{a}_{\ell n}^{(1,1)}$, $\tilde{b}_{\ell n}$, and $\tilde{c}_{\ell n}$, involved in Eq. (6.2b), are given by

$$\tilde{w}_n = \tilde{W}_n(x, z = 0), \tag{A.4}$$

$$\tilde{a}_{\ell n}^{(0,2)} = \langle \tilde{Z}_n, \tilde{W}_\ell \rangle_0 = \int_{z=-h(x)}^{z=0} \tilde{Z}_n(z; h) \tilde{W}_\ell(z; h) \mathrm{d}z, \tag{A.5a}$$

$$\tilde{a}_{\ell n}^{(1,1)} = -\frac{1}{2} [\tilde{Z}_n \tilde{Z}_\ell]_{z=0} = -\frac{1}{2}, \tag{A.5b}$$

$$\tilde{b}_{\ell n} = 2 \left\langle \frac{\partial \tilde{Z}_n}{\partial x}, \tilde{W}_\ell \right\rangle_0 + \frac{\partial h}{\partial x} [\tilde{Z}_n \tilde{W}_\ell]_{z=-h}, \tag{A.5c}$$

$$\tilde{c}_{\ell n} = \langle \Delta \tilde{Z}_n, \tilde{W}_\ell \rangle_0 + \left[\left(\frac{\partial h}{\partial x} \frac{\partial \tilde{Z}_n}{\partial x} + \frac{\partial \tilde{Z}_n}{\partial z} \right) \tilde{W}_\ell \right]_{z=-h} + \frac{1}{2} \left[\frac{\partial \tilde{Z}_\ell}{\partial z} \frac{\partial \tilde{Z}_n}{\partial z} \right]_{z=0}. \tag{A.5d}$$

References

[1] Andrianov AI, Hermans AJ. The influence of water depth on the hydroelastic response of a very large floating platform. Mar Struct 2003; 16:355–71.

[2] Athanassoulis GA, Belibassakis KA. A consistent coupled-mode theory for the propagation of small-amplitude water waves over variable bathymetry regions. J Fluid Mech 1999;389:275–301.

[3] Athanassoulis GA, Belibassakis KA. A coupled-mode, fully-dispersive, weakly-nonlinear model for water waves over a general bathymetry. In: Proc. 12th intern. offshore and polar conference and exhibition ISOPE 2002. 2002.

[4] Athanassoulis GA, Belibassakis KA. A nonlinear coupled-mode model for water waves over a general bathymetry. In: Proc. 21st international conference on offshore mechanics and arctic engineering OMAE 2002. 2002.

[5] Beji S, Nadaoka K. A time-dependent nonlinear mild-slope equation for water waves. Proc R Soc Lond A 1997;453:319–32.

[6] Belibassakis KA, Athanassoulis GA. Extension of second-order Stokes theory to variable bathymetry. J Fluid Mech 2002;464:35–80.

[7] Belibassakis KA, Athanassoulis GA. A coupled-mode model for the hydroelastic analysis of large floating bodies over variable bathymetry regions. J Fluid Mech 2005;531:221–49.

[8] Belibassakis KA, Athanassoulis GA, Gerostathis TP. A coupled-mode model for the refraction-diffraction of linear waves over steep three-dimensional bathymetry. Appl Ocean Res 2001;23:319–36.

[9] Coddington EA, Levinson N. Theory of ordinary differential equations. New York: McGraw Hill; 1955.

[10] Dingemans M. Water wave propagation over uneven bottoms. World Scientific; 1997.

[11] Eatock Taylor R, Ohkusu M, editors. J Fluid Struct 2000; 14 (7) [special issue].

[12] Ertekin CR, Kim JW, Yoshida K, Mansour AE, editors. Mar Struct 2000; 13 (4–5) [special issue]; Mar Struct 2001; 14 (1–2) [special issue].

[13] Faltinsen OM. Hydroelastic slamming. J Mar Sci Technol 2001;5(2).

[14] Fung YC. Foundations of solid mechanics. Prentice Hall; 1965.

[15] Gelfand IM, Fomin SV. Calculus of variations. Englewood Cliffs (New Jersey): Prentice-Hall; 1963.

[16] Greco M, Landri M, Faltinsen OM. Local hydroelastic analysis of VLFS with shallow draft. In: Proc. hydroelasticity in marine technology 2003. 2003.

[17] Hermans AJ. The ray method for the deflection of a floating flexible platform in short waves. J Fluid Struct 2003;17:593–602.

[18] Hermans AJ. A boundary element method for the interaction of free-surface waves with a very large floating flexible platform. J Fluid Struct 2000;14:943–56.

[19] Hong SY, Kim JW, Ertekin RC, Shin YS. An eigenfunction expansion method for hydroelastic analysis of a floating runway. In: Proc. 13th international offshore and polar conference and exhibition conference ISOPE 2003, vol. 1. 2003. p. 121–8.

[20] Kashiwagi M. A B-spline Galerkin scheme for calculating the hydroelastic response of a very large structure in waves. J Mar Sci Technol 1998;3:37–49.

[21] Kashiwagi M. Research on hydroelastic responses of VLFS: Recent progress and future work. J Offshore Polar Eng 2000;10(2):81–90.

[22] Kim JW, Ertekin RC. An eigenfunction expansion method for predicting hydroelastic behavior of a shallow-draft VLFS. In: Kashiwagi et al., editors. Proc. hydroelasticity in marine technology. Kyushu University (Fukuoka, Japan): RIAM; 1998. p. 47–59.

[23] Kim JW, Ertekin RC. Hydroelasticity of an infinitely long plate in oblique waves: linear Green Naghdi theory. J Eng Mar Environ 2002;216(M2): 179–97.

[24] Kyoung JH, Hong SY, Kim BW, Cho SK. Hydroelastic response of a very large floating structure over a variable bottom topography. Ocean Eng 2005;32:2040–52.

[25] Liu PL-F. Model equations for wave propagation from deep to shallow water. In: Liu PL-F, editor. Advances in coastal and ocean engineering. World Scientific; 1995.

[26] Luke JC. A variational principle for a fluid with a free surface. J Fluid Mech 1967;27:395–7.

[27] Magrab EB. Vibrations of elastic structural members. The Netherlands: Sijthoff & Noordhoff; 1979.

[28] Massel S. Extended refraction-diffraction equations for surface waves. Coastal Eng 1993;19:97–126.

[29] Marchenko AV, Shrira VI. Theory of two-dimensional nonlinear waves in liquid covered by ice. Izv Akad Nauk SSSR Mekh Zhidk I Gaza 1991; 4:125–33.

[30] Murai M, Inoue Y, Nakamura T. The prediction method of hydroelastic response of VLFS with sea bottom topographical effects. In: Proc. 13th ISOPE conference. 2003. p. 107–12.

[31] Nagata S, Niizato H. Variational principles related to motions of an elastic floating plate in nonlinear water wave. In: Proc. 12th international offshore and polar conference and exhibition conference ISOPE 2002, vol. 1. 2002. p. 350–7.

[32] Nadaoka K, Beji S, Nakagawa Y. A fully dispersive weakly nonlinear model for water waves. Proc R Soc Lond A 1997;453:303–18.

[33] Ohkusu M, Namba Y. Analysis of hydroelastic behavior of a large floating platform of thin plate configuration in waves. In: Proc. international workshop on very large floating structures. 1996. p. 143–8.

[34] Porter D, Porter R. Approximations to wave scattering by an ice sheet of variable thickness over undulating bed topography. J Fluid Mech 2004; 509:145–79.

[35] Shiraishi S, Iijima K, Yoneyama H. Elastic response of a very large floating structure in waves moored inside a coastal reef. In: Proc. 12th international offshore and polar conference and exhibition conference ISOPE 2002, vol. 1. 2002. p. 327–34.
[36] Smith R, Sprinks T. Scattering of surface waves by a conical island. J Fluid Mech 1975;72:373–84.
[37] Squire VA, Dugan JP, Wadhams P, Rottier PJ, Liu AK. Of ocean waves and ice sheets. Ann Rev Fluid Mech 1995;27:115–68.
[38] Takagi K, Shimada K, Ikebuchi T. An anti-motion device for a very large floating structure. Mar Struct 2000;13:421–36.
[39] Tkacheva LA. Hydroelastic behaviour of a floating plate in waves. J Appl Mech Tech Phys 2001;42(6):991–6.
[40] Utsunomiya T, Watanabe E, Nishimura N. Fast multipole algorithm for wave diffraction/radiation problems and its application to VLFS in variable water depth and topography. In: Proc. 20th international conference on offshore mechanics and arctic engineering, vol. 7. 2001. p. 1–7. Paper 5202.
[41] Wang CD, Meylan MH. The linear wave response of a floating thin plate on water of variable depth. Appl Ocean Res 2002;24:163–74.
[42] Watanabe E, Utsunomiya T, Wang CM. Hydroelastic analysis of pontoon-type VLFS: a literature survey. Engineering Structures 2004;26:245–56.
[43] Witham GB. Linear and nonlinear waves. New York: Wiley; 1974.
[44] Zakharov VE. Stability of periodic waves of finite amplitude on the surface of a deep fluid. J Appl Math Tech Phys 1968;2:190.